Manuscript: acp-2016-730

Editor comment:
I received three evaluations of your revisions. Overall, all three reviewers feel that the paper can be further enhanced and that the replies to the reviews should be improved. I urge you to put a substantial effort in enhancing the paper and answer to each of the points that in the Reviewers' comments thoroughly.

Response:
The authors thank the reviewers for interest in our work and for the helpful comments to improve the manuscript. We have addressed and incorporated the points raised and we appreciate the invitation by the editor to resubmit the article following revision.

Please note that all page and line numbers refer to the revised manuscript and the revised supplementary material with track changes. Author's responses are in italics and text colored in red refers to the added text in the manuscript.

Author response to Referee #2

This paper has been greatly improved after the first revision. After reading through the revised paper and response, a minor revision was considered here.

Major comments:

Comment 1:
To response 6: The addressing here is quite right. The dilution will not change the f44/f60 ratios assuming the variation of volatility due to dilution will not change the SOA/BBOA fraction very much. However, the mixing with other plumes which contains comparable or higher OA mass concentration compare to BB plumes, will greatly change the f44/f60 ratio. E.g., If the biomass burning plumes mixed with the biogenic dominated air mass, f60 will decrease and f44 is possibly going to change as well.

Although the authors added the possibility of dilution effect in the explanation, the sentence is not in a proper position (originally in last sentence in the first paragraph of page 10), should be mentioned in the f44 vs f60 explanation of Page 9 line 19 to 21 and other relevant places.

Response 1:
The authors agree with the referee's comment. The sentence adding the possibility of dilution effect (in more clear form): "One more factor that can influence the f44 vs f60 trend for both close and distant fire is mixing of the BB plume with air masses containing aerosol particles from other sources (dilution effect)" is relocated from Page 10, line 7 to Page 9, lines 21 and 22.

Comment 2:
a) For the whole 3.2.2 section. I did not see the meaning of this paragraph. The ΔOA/ΔCO cannot be used for the SOA formation since the ΔOA/ΔCO (ΔOA or ΔCO) from different fresh BB plumes can vary within a wide range (more than a factor of 10) depending on combustion material, condition etc. E.g., (Aiken et al., 2009). The authors do not know ΔOA/ΔCO from different fresh BB plumes surround this observation site are constant or not. And mixing with fresh or aging plumes from other fires or plumes is possible, which will change the initial ΔOA/ΔCO ratio. I suggest to delete this part.

b) Similar comment also applies to 3.2.1 section $\Delta O_3/\Delta CO$. The initial $\Delta O_3/\Delta CO$ is unknown or the authors should give the range of $\Delta O_3/\Delta CO$ for fresh BB plume.

Response 2:
a) The authors agree that not enough data are available for the conclusions regarding the SOA formation (ΔOA/ΔCO diurnal trend analysis). Therefore, the authors removed this part (Page 11, line 1 to Page 11 line 12) from the revised manuscript, as suggested. Figure 5 that corresponds to the removed text was also removed from the revised manuscript version (Page 26). The first part of the 3.2.2 section which says "Since increased photochemical activity was identified in BB air masses, the change in ΔOA/ΔCO ratio was investigated in order

to determine whether additional OA was produced in the BB plumes (Fig. 4e and Fig. 4f). The lowest OA concentration observed during the campaign of 0.09 µg m^{-3} *was taken as a background value in these calculations. Figures show no particular trend in* $\Delta OA/\Delta CO$ *ratio with f44. The* $\Delta OA/\Delta CO$ *ratio remains quite constant despite increases in f44 (Fig. S5)" was moved to the end of the previous section 3.2.1 (Ozone formation). This part illustrates that there is no particular trend observed, considering all sampled plumes on whether the aging leads to additional OA generation, due to number of different plume masses.*

b) Although the initial value for the $\Delta O_3/\Delta CO$ *is unknown, here the authors are considering the overall trends, more precisely ozone enrichments with aging (f44 increase) for close and distant emissions and comparison of the average* $\Delta O_3/\Delta CO$ *ratio between close and distant fires. The trends are clearly showing higher photochemical activity with more aged masses. Therefore the paragraph is kept in the manuscript.*

Comment 3:
Section 3.2.4 (the biomass burning events) is too long. There is too much unnecessary detailed information from each fire. Please shorten this section (cut or move some information to the supplementary materials) and give the necessary conclusion. I did not see the scientific points that the authors want to address here.

Response 3:
The authors agree and the Section 3.2.4 is shortened. The details about the sentinel hotspots detected on days of biomass burning events, including fire confidence level and location, are moved to the supplementary information (Page 4 and 5 within the Sect S2.2). Some corrections were made throughout the section and more conclusions are made at Page 14, lines 4-13:"In summary, the backtrajectory analysis showed that not more than half an hour was needed for the air masses to reach the ATARS from each area affected by close fire events. All sampled aerosols had f44 values lower than 0.1, which likely reflects fresher aerosol masses. Only aerosols emitted from Event F had higher f44 values, which can be a reflection of aerosol processing but also different factors, including mixing of masses due to the abrupt wind changes. The variation between fires and their burning material and conditions, can also be seen through a wide range of MCE values, from 0.9 to 0.98. Events were characterised with different f60/f73 ratios (varying between 1.2 and 2.5), and there was no trend in the relationship between f60/f73 ratio and burning material/conditions (MCE values) (Fig. S8). In general, the diversity of BB plumes was illustrated through high variability in chemical signature as a product of different burning conditions/material for these five intense fire events". The sentence that emphasise the variability of five fire events and how comprehensive approach and more dataset has to be taken is given in the Conclusion at Page 17, lines 23-25: "Even across these five events, the chemical signature varied significantly (e.g. wide range in f44, from 0.06 to 0.18) which emphasises the need for a more comprehensive dataset that characterises the factors associated with burning material, conditions and processing".

Minor comments:

Comment 1:
The definition of organics is very wide, which can also refer to gas-phase organics. Please use the abbreviation "OA" instead of "organics" when referring to organic aerosol to avoid confusion.

Response 1:
The abbreviation "OA" is used instead of "organics" when referring to organic aerosol.

Comment 2:
Page5 Line 16: add abbreviation name of "(OOA)" after "oxygenated OA"

Response 2: The abbreviation "OOA" is written after the "Oxygenated OA" at Page 5, line 17 of the revised manuscript.

Comment 3:
Page 16 line 20 not only "the influence of BB emissions", but also "the aged SOA from different sources." Can influence this f82 ratio.

Response 3:
The suggested modification is made to the manuscript at Page 17, lines 2-4: "The lower value for SAFIRED compared to Borneo forest, considering that biogenic influence is significant for both environments, can be attributed to the high influence of BB emissions but also to the aged SOA that are from different sources".

Author response to Referee #1

Comment 1:

I thank the authors for taking time to revise the manuscript. The authors have addressed the comments adequately.

However, I have one minor comment. In response#2 to reviewer#1 (and corresponding places in the revised manuscript), please remove or rephrase the sentence “In order to estimate whether the acidity of the particles had an influence on isoprene-derived OA generation in ATARS, the correlation between sulfate (taken as proxy of aerosol acidity) and isoprene-derived OA factor was examined.” This is because sulfate influences isoprene-derived OA through multiple ways (particle acidity, volume, surface area, liquid water, etc) and sulfate cannot be taken as proxy of aerosol acidity.

Response 1:

The authors agree that sulfate can influence isoprene through multiple ways and cannot be taken simply as a proxy of aerosol acidity. Therefore, the paragraph is removed from the manuscript at Page 15 of the revised manuscript and Figure S18 (Page 15 of the supplementary information) that corresponds to the paragraph was removed as well.

Author response to Referee #3

Comment 1: While I thank the authors for revising the title, it is still exclusively biomass burning focused, which does not reflect the content of the paper.

Response 1: Authors agree with the comment. Title has been rephrased for “Biomass burning and biogenic aerosols in northern Australia during the SAFIRED campaign”.

Comment 2: The response regarding the increase in isoprene SOA in response to the boundary layer height is not adquate. For isoprene to build up during a nocturnal inversion it must be continuously emitted, however biogenic isoprene is generally only emitted during the day. I would expect that a different mechanism is reponsible, such as a change in wind sector or partitioning of semivolatile species, but the PTR-MS should indicate one way or another whether an increase in precursor concentrations is responsible.

Response 2: The authors think that the isoprene doesn’t have to be necessarily emitted continuously for isoprene oxidation products to partition over the night. The lower boundary layer is “concentrating” the gases inducing the partitioning of gaseous compounds including the low volatility isoprene-derived OA. To make this more clear, the paragraph (Page 16, lines 14-20) is modified: “This night-time enhancement might be due to transport of distant air masses, or partitioning of lower volatility species into the particle phase as the temperature drops and relative humidity increases, as suggested by Budisulistiorini et al. (2013). In addition, the boundary layer height becomes lower during the night, increasing the concentration of gaseous compounds. This boundary layer reduction might induce low volatility OA partitioning, contributing to the increase in isoprene-derived OA”.

Comment 3: Regarding the dOA/dCO analysis vs time of day, it would be useful to state the estimated plume ages here, based on HYSPLIT and the MODIS data. This would give an indication of how meaningful the diurnal profiles are likely to be.

Response 3: The part regarding the SOA formation (ΔOA/ΔCO analysis) is removed from the manuscript (Page 11, line 1 to Page 11 line 12), as suggested by the Referee #2 and due to insufficient data for further *conclusions. Figure 5 that corresponds to the removed text was also removed from the revised manuscript version (Page 26). The first part of the section which says "Since increased photochemical activity was identified in BB air masses, the change in ΔOA/ΔCO ratio was investigated in order to determine whether additional OA was produced in the BB plumes (Fig. 4e and Fig. 4f). The lowest OA concentration observed during the campaign of 0.09 µg m-3 was taken as a background value in these calculations. Figures show no particular trend in ΔOA/ΔCO ratio with f44. The ΔOA/ΔCO ratio remains quite constant despite increases in f44 (Fig. S5)"was moved to the end of the previous section 3.2.1 (Ozone formation). This part illustrates that there is no particular trend observed considering all sampled plumes on whether the aging leads to additional OA generation, due to number of different plume masses.*

~~Fresh and aged aerosols emitted from biomass burning in northern Australia~~Biomass burning and biogenic aerosols in northern Australia during the SAFIRED campaign

Andelija Milic[1], Marc D. Mallet[1], Luke T. Cravigan[1], Joel Alroe[1], Zoran D. Ristovski[1], Paul Selleck[2], Sarah J. Lawson[2], Jason Ward[2], Maximilien J. Desservettaz[3], Clare Paton-Walsh[3], Leah R. Williams[4], Melita D. Keywood[2], Branka Miljevic[1]

[1]International Laboratory for Air Quality and Health, Queensland University of Technology, Brisbane, Queensland, 4000, Australia
[2]CSIRO Oceans and Atmosphere, Aspendale, Victoria, 3195, Australia
[3]Centre for Atmospheric Chemistry, University of Wollongong, Wollongong, New South Wales, 2522, Australia
[4]Aerodyne Research, Inc., Billerica, Massachusetts, 01821, USA

Correspondence to: Branka Miljevic (b.miljevic@qut.edu.au)

Abstract. There is a lack of knowledge of how biomass burning aerosols in the tropics age, including those in the fire-prone Northern Territory in Australia. This paper reports chemical characterization of fresh and aged aerosols monitored during the one month long SAFIRED (Savannah Fires in the Early Dry Season) field study, with an emphasis on the chemical signature and aging of organic aerosols. The campaign took place in June 2014 during the early dry season when the surface measurement site, the Australian Tropical Atmospheric Research Station (ATARS), located in the Northern Territory, was heavily influenced by thousands of wild and prescribed bushfires. ATARS was equipped with a wide suite of instrumentation for gaseous and aerosol characterization. A compact time-of-flight aerosol mass spectrometer was deployed to monitor aerosol chemical composition. Approximately 90 % of submicron non-refractory mass was composed of organic material. Ozone enhancement in biomass burning plumes indicated increased air mass photochemistry~~ and increased organic aerosol with the aging parameter (f44) suggested secondary organic aerosol formation~~. ~~Diversity ~~The diversity ~~of ~~in biomass burning emissions was illustrated through variability in chemical signature (e.g. wide range in f44, from 0.06 to 0.18) for five intense fire events. The background particulate loading was characterized using Positive Matrix Factorization (PMF). A PMF-resolved BBOA (biomass burning organic aerosol) factor comprised 24 % of the submicron non-refractory organic aerosol mass, confirming the significance of fire sources. A dominant PMF factor, OOA (oxygenated organic aerosol), made up 47 % of the sampled aerosol~~ fraction~~, illustrating the importance of aerosol aging in the Northern Territory. Biogenic isoprene-derived organic aerosol factor was the third significant fraction of the background aerosol (28 %).

Keywords. Biomass burning, savannah fires, organic aerosol, aerosol aging

1 Introduction

Tropical regions are some of the most fire-prone areas in the world (Crutzen and Andreae, 1990). As one of them, Northern Australia is observed to be a significant contributor to the global biomass burning (BB) budget (Russell-Smith et al., 2007). Fire emissions are made up of a variety of gaseous and particle-phase species, with the particle-phase consisting primarily of carbonaceous particles, including organic carbon (OC) and elemental carbon (EC) (Bond et al., 2004;Hallquist et al., 2009;Formenti et al., 2003;Crutzen and Andreae, 1990). Open fires are the largest contributors to carbonaceous emissions; approximately 70 % and 40 % of the global annual emissions of OC and EC are formed in open fire events, respectively (Bond et al., 2004). Annually, 60-75 % of Australia's carbon emissions are attributed to BB emissions in tropical savannahs (Hurst et al., 1994). Organic carbon and EC affect the Earth's radiation balance by scattering and absorbing solar radiation, respectively (Penner et al., 1998;Haywood and Boucher, 2000). O'Brien and Mitchell (2003) suggested that atmospheric heating caused by UV absorbing carbonaceous aerosol, related to BB events in the Northern Territory during a dry season, can be significant and will likely have an influence on local (and possibly even global) climate. Carbonaceous species can also serve as condensation nuclei in cloud formation processes (Roberts et al., 2002). It is therefore important to build a comprehensive knowledge of BB emissions as they play a key role in the climate.

The characterization, processing and estimation of impact of BB emissions is a complex and challenging issue due to a wide range of burning material and combustion conditions (flaming/smouldering), as well as complex atmospheric physics and chemistry that BB plumes undergo once emitted (Reid et al., 2005;Weimer et al., 2008). Besides the characterization of fresh BB emissions, it is important to address their evolution in the atmosphere since aging of the BB emissions will alter their properties and thus how they interact with the climate system. Fresh BB emissions are those released directly from BB sources, while processed emissions refer to fresh particle or gaseous species transformed in the atmosphere through photochemical processing (aging). Organic aerosols (OA) can be differentiated as directly emitted primary organic aerosols (POA), aged primary organic aerosols (aged POA) and secondary organic aerosols (SOA) that form via condensation of lower volatility photo-oxidation products. A large fraction of BB-related POA is observed to be semivolatile (Grieshop et al., 2009) and can therefore change upon dilution with background air by evaporation of its content into the gas phase and be exposed to further transformations in the atmosphere.

Processing of BB emissions in the ambient atmosphere and in laboratory experiments is characterized by increases in the oxygenated fraction of OA (OOA) and degradation of species that are indicators of BB origin (Cubison et al., 2011;DeCarlo et al., 2008;Capes et al., 2008). However, there is no agreement on whether the aging of BB emissions leads to additional OA production. Some recent field and laboratory studies investigating the evolution of BB plumes have shown that OA mass increases with aging (DeCarlo et al., 2008;Yokelson et al., 2009;Heringa et al., 2011), while others have found no significant change or a decrease in OA with atmospheric processing (Akagi et al., 2012;Brito et al., 2014;Cubison et al., 2011;Capes et al., 2008). In addition to SOA formation, BB plumes promote the production of another important secondary pollutant, tropospheric ozone (Real et al., 2007). An excess of nitrogen oxides (NO_X), non-methane organic compounds (NMOCs) and carbon monoxide (CO) in the atmosphere from fire emissions promote additional pathways for ozone production (Parrington et al., 2013). Ozone enhancement in BB emissions has been extensively used as a proxy for air mass photochemical activity (Hobbs et al., 2003;Jaffe and Wigder, 2012;Yokelson et al., 2009;Akagi et al., 2012).

An extensive area of the Northern Territory of Australia is burned each year during the dry season (May-October) and the region is strongly affected by BB emissions. Considering that this area is a globally significant source of BB aerosol emissions (Mitchell et al., 2013), and that there have been a limited number of studies on aerosol characterization and aging, there is a need for more research. Information about the composition and degree of aging of the OA that makes up the majority of emitted species generated in these fires will facilitate the estimate of the influence of BB in the Northern Territory. This will also contribute to a better understanding of fire emissions in tropical regions. In order to address these issues, the one month long SAFIRED (Savannah Fires in the Early Dry Season) field study was conducted at the Australian Tropical Atmospheric Research Station (ATARS) during a frequent burning period (late May/June 2014). This publication presents insights into fresh and aged aerosols emitted during the SAFIRED, while a detailed description of the campaign can be found in Mallet et al. (2016).

2 Measurement site and period

The ~~Australian Tropical Atmospheric Research Station (~~ATARS~~)~~ is situated on the Gunn Point peninsula in the Northern Territory (12°14'56.6" S, 131°02'40.8" E). The northern Australian tropical land mass is mostly covered by savannah biomes including scattered eucalypt trees, shrubs and grasses (Lacey et al., 1982). The sampling site can be described as rural background due to its remote location, with the closest populated centre, the city of Darwin, approximately 80 km south west of the ATARS. During the measurement period, the dominant sources of gaseous and aerosol species were wild and prescribed fires. Apart from planned burns, anthropogenic inputs to this region can be considered negligible (Bowman et al., 2007) and observations have highlighted the importance of biogenic sources for this area (Allen et al., 2008). The sampling site can also be impacted by marine aerosols (Bouya et al., 2010); however, fires are the major source of aerosols during the dry season.

The SAFIRED campaign was conducted from the 29th of May until the 30th of June, 2014 at the beginning of the dry season. The early dry period is characterized by natural fires as well as prescribed burns conducted to reduce the extent, intensity and frequency of wildfires in the late dry season (October-November). Thousands of fires in the Northern Territory during the campaign were detected by MODIS and VIIRS satellite sensors (Mallet et al., 2016). Fire emissions sources ranged from approximately two to up to hundreds of kilometres distant from the sampling station.

The early dry season was characterized by dry weather conditions (average relative humidity of 67 ± 23 %) and warm days with an average daily and nightly temperatures of 27 ± 5 °C (up to 34 °C) and 19 ± 4 °C (with a minimum of 10 °C), respectively. There were no days of rainfall. Wind direction was predominantly southeast, suggesting that the sampled air masses had mainly passed over land affected by fire emissions. However, on some days (e.g. between the 3rd and 6th of June) in the afternoon hours the northeast wind direction was dominant, directing the air masses from land to pass over the ocean before being detected at ATARS. Moreover, an oceanic influence was observed between the 19th and 22nd of June (Mallet et al., 2016).

2.1 Instrumentation and method

Ground level characterization was performed using a wide range of instrumentation for gas- and particle-phase measurements. Detailed description of all instruments used in SAFIRED is given in Mallet et al. (2016). The focus of this study was on the aerosol chemical composition and aging using the instrumentation listed in the following paragraphs.

2.1.1 Compact Time-of-Flight Aerosol Mass Spectrometer (cToF-AMS)

A compact time-of-flight aerosol mass spectrometer (cToF-AMS or AMS, Aerodyne Research, Inc.) was deployed to monitor the chemical composition of non-refractory submicron (PM_1) aerosol. Monitored species were submicron particulate ~~organic~~ OA and inorganic compounds (sulfate, ammonium, nitrates and chlorides). Details about instrument operation during this campaign can be found in Mallet et al. (2016).

Unit mass resolution (UMR) and high resolution (HR) AMS data analysis was performed in Wavemetrics Igor Pro software (version 6.36) using the standard AMS Analysis Toolkits, Squirrel (Version 1.56D) and PIKA (Version 1.16), respectively. Data collection with a filter at the instrument inlet was used to correct for contributions from air in the fragmentation table (Aiken et al., 2008). Measured time-resolved gas-phase CO_2 concentrations were applied instead of the fragmentation table default value. The AMS collection efficiency was determined using the calculations provided within the PIKA Toolkit. The composition dependent collection efficiency panel enables an estimate of the collection efficiency based on ammonium nitrate, ~~organic~~ OA content, aerosol acidity and relative humidity (Middlebrook et al., 2012). The time-resolved collection efficiency (with an average value of 0.61) was applied to the entire dataset. High OA loadings during the campaign caused interferences in the detection of sulfate in the UMR analysis. Significant improvement was made in distinguishing sulfate fragments from ~~organic~~ OA fragments at the same m/z by performing HR peak fits in PIKA (Sect. S1 in supplementary information). Therefore, HR peak fitting data (PIKA) were chosen for further analysis.

AMS fragments analysis

Organic aerosols measured by the AMS encompassed aerosols that were processed in the atmosphere for different periods of time and included both POA and SOA. As such, a tool was needed to distinguish BB aerosol from other sources and fresh from processed BB aerosol. An extensively employed fragments analysis using the AMS-extracted parameters f43 (ions $C_3H_7^+$ and $C_2H_3O^+$), f44 (CO_2^+) and f60 ($C_2H_4O_2^+$) was applied here. The ratio of an integrated organic signal, e.g. m/z 43, to total organic signal is referred to as f43. Parameters f43 and f44 were used to estimate the level of OA processing, as they illustrate OA fractions of different aging degree. While f43 is mainly associated with hydrocarbon-like and semivolatile OA fractions (fragments $C_3H_7^+$ and $C_2H_3O^+$, respectively) (Jimenez et al., 2009;Lanz et al., 2007;Zhang et al., 2007;Heringa et al., 2011), f44 is assigned to highly oxygenated OA species (fragment CO_2^+) (Aiken et al., 2007;DeCarlo et al., 2010;Alfarra et al., 2007). The AMS parameter f60 and accompanying f73 ($C_3H_5O_2^+$) are widely used as BB emission signatures as they are directly related to levoglucosan-like species, which are a substantial fraction of organics emitted in pyrolysis of cellulose (Alfarra et al., 2007;Simoneit et al., 1999). The f60 can be applied as a valuable BB marker for time periods of up to one day (Cubison et al., 2011;Bougiatioti et al., 2014). Ambient aerosols characterized by an f60 value higher than 0.003 are considered to be influenced by BB emissions (Cubison et al., 2011). A graphical approach of comparing f44 vs. f60 introduced by Cubison et al. (2011) was used in this study to estimate the degree of aging of BB emissions.

Positive Matrix Factorization (PMF)

Positive Matrix Factorization (PMF) analysis (Paatero and Tapper, 1994) using the PMF evaluation tool (Ulbrich et al., 2009) was used in source apportionment of the AMS OA data. PMF splits the OA spectrum into different factors that can be related to specific sources (Paatero, 1999;Paatero and Hopke, 2009). Various factors have been identified by PMF analysis of AMS OA data, with the most common being hydrocarbon-like OA (HOA) and oxygenated OA (OOA), that can sometimes be further apportioned to low-volatility oxygenated OA (LV-OOA) and semivolatile oxygenated OA (SV-OOA) (Ulbrich et al., 2009;Lanz et al., 2007;Ng et al., 2010;Jimenez et al., 2009). Other factors include environment specific factors such as biomass burning OA (BBOA) and cooking-related OA (COA). The solution space in this study was investigated by varying the number of factors and starting conditions (seeds, 0 to 50 in increments of 1) and applying rotational parameters (fpeaks, -1 to 1 in increments of 0.1).

2.1.2 Beta plus particle measurement system (BAM)

PM_1 mass was measured and collected onto pre baked (600 °C) quartz 47 mm filters (Pall Tissuquatz p/n 7202) using a Beta plus particle measurement system (BAM, Teledyne API Model 602), every 12 hours. All of the species measured on BAM filters were blank corrected. Particles collected on filters were further analysed for anhydrous sugars, including levoglucosan, by high performance anion exchange chromatography with pulsed amperometric detection and for water soluble ions including potassium (K^+), nitrates (NO_3^-), sulfates (SO_4^{2-}), ammonium (NH_4^+) and chlorides (Cl^-) by ion suppressed chromatography. Levoglucosan and non-sea salt K^+ were used as metrics for BB emissions. BAM PM_1 filters were analysed by a Thermal-Optical Carbon Analyser (DRI Model 2001A) using the IMPROVE-A temperature protocol (Chow et al., 2007) to determine contributions of EC and OC. Water soluble inorganic ions and OC were also used for comparison with AMS-resolved species.

2.1.3 Fourier Transform Infrared Spectrometer (FTIR)

The Spectronus trace gas and isotope Fourier Transform Infrared Spectrometer (FTIR) analyser, built by the Centre of Atmospheric Chemistry at the University of Wollongong, was deployed to monitor gaseous species including carbon monoxide (CO) and carbon dioxide (CO_2) (Griffith et al., 2012;Griffith, 1996). Details about the instrument operation can be found elsewhere (Desservettaz et al., 2016). In order to include dilution effects, OA and ozone data are presented relative to CO. CO is an important BB product that can remain in the atmosphere for a relatively long time period (one to two months depending on the environment) without observed decay or interactions with oxidative agents (Wang and Prinn, 1999;DeCarlo et al., 2010;Edwards et al., 2006). CO has therefore been employed as a long-lived, conservative tracer in many studies (DeCarlo et al., 2010;Kleinman et al., 2008;Brito et al., 2014;Yokelson et al., 2009;Akagi et al., 2012). Gas-phase CO_2 data, as previously mentioned, were applied in the AMS fragmentation table adjustment. CO and CO_2 were also used in modified combustion efficiency (MCE) calculations, with details presented in Desservettaz et al. (2016). MCE refers to the ratio of ΔCO_2 (measured value relative to background value) to the sum of ΔCO_2 and ΔCO (Ward and Radke, 1993). The MCE parameter was used to distinguish smouldering (usually lower than 0.9) from flaming (usually higher than 0.9) fires. The MCE value can also indicate the burning material.

2.1.4 Scanning Mobility Particle Sizer (SMPS)

Aerosol size and number concentration were monitored by a Scanning Mobility Particle Sizer (SMPS, a TSI 3071 long-column electrostatic classifier coupled to a TSI 3772 Condensation Particle Counter). The SMPS measured the particle size distribution from 14 nm up to 670 nm every 5 minutes. Changes in the size distribution due to aging were investigated.

2.1.5 Proton Transfer Reaction-Mass Spectrometer (PTR-MS)

A high sensitivity Proton Transfer Reaction-Mass Spectrometer (PTR-MS, Ionicon Analytik) with a quadrupole mass spectrometer and an H_3O^+ ion source was employed to measure non-methane organic compounds (NMOCs) that include non-methane hydrocarbons and oxygenated volatile organic compounds. These species are important in the formation of SOA and ozone. Isoprene and monoterpenes make up a dominant fraction of global gas-phase NMOCs, contributing significantly to the production of SOA (Guenther et al., 2012). Tropical regions can contribute up to 80 % of global annual isoprene emissions due to warm weather conditions (Guenther, 2006). He et al. (2000) investigated NMOCs emitted from eucalyptus trees, which make up 95 % of all tree species in Australia. Isoprene accounts for 64-100 % of NMOCs emitted from different eucalyptus species. The isoprene/furan fraction (signal at m/z 69) of measured NMOCs is used here in the analysis of isoprene-derived OA. Other studies suggest that the contribution of isoprene to m/z 69 prevails in non-BB periods while the furan contribution is more significant in BB plumes (Warneke et al., 2011). In order to distinguish furan and isoprene contribution over the sampling period, a gas chromatography-mass spectrometry method was used.

2.1.6 Ozone analyser

Ozone concentration was monitored by an Ultraviolet Photometric Ozone analyser (Model 49i, Thermo Scientific). Ozone enhancement in BB emissions has been used as a proxy for air mass photochemical activity.

2.1.7 Fire data

Information about the location and duration of fires was obtained from the Sentinel Hotspots system. Hotspots data used for this campaign were derived from the MODIS (Moderate Resolution Imaging Spectroradiometer) sensor (Terra and Aqua satellites) and VIIRS (Visible Infrared Imaging Radiometer Suite) sensor (Suomi NPP satellites). Only the hotspots with confidence level higher than 50 % were considered in the analysis. Hotspots are detected by satellite once a day which limited the fire analysis to events that occurred between approximately 11 am and 3 pm. During the SAFIRED campaign thousands of fires were detected in the Northern Territory. Distance-resolved fire frequencies are presented in Mallet et al. (2016). Moreover intense fires characterized by plumes detected without considerable influence from other fire sources, were extracted from the whole dataset (Desservettaz et al., 2016). Five events that were categorised as single, intense fires are analysed here. Air mass backtrajectories were computed using the NOAA/ARL HYSPLIT (Hybrid Single-Particle Lagrangian Integrated Trajectory) model.

3. Results and Discussion

3.1 Aerosol chemical characterization

PM_1 ambient aerosols sampled during the SAFIRED campaign were dominated by an ~~organic~~ OA fraction. Organic carbon made up 72 % and EC 15 % of the measured PM_1 on the BAM filters (Fig. 1a). Data from the AMS (Fig. 1b and 1c), indicate that ~~organics~~ OA made up approximately 90 % of submicron non-refractory mass with an average concentration of 11.1 µg m^{-3} and concentrations of up to 350 µg m^{-3} during intense and nearby BB events. The ~~organic mass (OM) sampled by~~OC from the BAM filters was converted ~~from Oc~~to organic mass (OM) using ~~the~~ a conversion factor of 1.4~~, (~~determined from analysis of the AMS OC and OM measurements (in PIKA). This value is within the span of OM/OC conversion factors for the BB aerosol suggested by Reid et al. (2005). The BAM OM and OA mass concentration ~~of organics~~ sampled by the AMS are in good agreement (R value of 0.94), with slightly higher concentrations measured by the BAM (Fig. S2c) probably due to the lower collection efficiency of the AMS above 700 nm. Organic mass has been observed to be the dominant fraction of PM_1 ambient aerosols during the early dry season in the Northern Territory (Carr et al., 2005). The ~~organic~~ OA fraction was also dominant in other studies strongly impacted by BB emissions (Brito et al., 2014;Capes et al., 2008). In this study, the remaining submicron non-refractory mass was made up of inorganics, including sulfates (4.2 %), ammonium (2.8 %), nitrates (1.5 %) and chlorides (1.3 %), with average concentrations of 0.51 ± 0.32 µg m^{-3}, 0.35 ± 0.68 µg m^{-3}, 0.19 ± 0.45 µg m^{-3} and 0.17 ± 1.28 µg m^{-3}, respectively.

The sampling site was constantly impacted by fire emissions with periods of heavy BBs characterized by high aerosol and gas phase concentrations, for instance CO reaching up to ~10^4 ppb and ~~organics~~ OA up to 350 µg m^{-3} (Fig. 2). The most intense BB episodes were on the 30th of May, between the 7th and 11th of June, and on the 25th and 26th of June (Mallet et al., 2016). During intense fire periods, ~~organics~~OA, CO and particle number concentration showed correlated increases (Fig. 2). Moreover, looking at Sentinel Hotspots during these periods, hot spots were detected within 20 km of the ATARS. Based on this, the dataset was separated into periods of “close BB” (corresponding to high ~~organics~~OA, CO and particle number concentration signals and close events (< 20 km)) and “distant BB” (corresponding to less intense ~~organics~~OA, CO and particle number concentration signals and distant events (> 20 km)). It is important to emphasize that all periods during the measurement campaign that have not been included in close BB periods have been assigned to distant BB periods, as ATARS was constantly influenced by BBs. The selection does not mean that emissions from distant fires were not present during the close BB periods but that the influence of fires near the measurement station during these periods was dominant. Nine intense BB events were identified from close BB periods as single source emissions (Desservettaz et al., 2016). Five of the nine events (Fig. 2) were analysed here (Sect. 3.2.~~4~~3), due to the instrument not sampling during the remaining events. Most of the events occurred in the afternoon/night time (Table 1).

Coupled with elevated ~~organic~~ OA concentrations, AMS-measured inorganics also increased during close BB periods (Fig. 1c). A high AMS signals for all monitored species corresponded to close BB periods. During SAFIRED, high correlation was observed between ~~organics~~ OA and ammonium species (R of 0.92), with better agreement during the close BB (R of 0.92) than in the distant BB periods (R of 0.73) (Table S1), suggesting that these ammonium species originated from fire emissions. Moreover, plume emissions included high chloride concentrations (up to approximately 50 µg m^{-3} during close BB periods). Increased chloride concentration during the close BB periods was also indicated by the BAM data (Fig. S3a). This is not surprising since the dominant fine particle inorganic fraction emitted in flaming savannah fires has been shown to be composed of KCl (potassium chloride) and NH_4Cl (ammonium chloride) compounds and/or their mixtures (Liu et al., 2000). There was a better correlation between ~~organics~~ OA and chlorides for close BB periods (R of 0.67), than for distant BB periods (R of 0.47). This can be explained by the depletion of chloride with transport and aging of BB plumes (Li et al., 2003;Li et al., 2010;Liu et al., 2000). Correlations for nitrate and sulfate with ~~organics~~ OA show similar patterns in this work regardless of the BB emissions influence (R of 0.72 and 0.77 for nitrate and R of 0.49 and 0.48 for sulfate for close and distant periods, respectively). AMS inorganic species were compared to soluble ions concentrations measured on the filter samples collected using the BAM. There was a strong correlation between all compared species (R values of 0.85, 0.68 and 0.81 for sulfates, ammonium and nitrate, respectively) except in the case of chloride (R of 0.18) (Fig. S2). Mg^{2+}/Na^{+} ratio values for the filters collected during the high oceanic influence (between the 3rd and 6th and the 19th and 22nd of June) were close to the sea salt Mg^{2+}/Na^{+} ratio of 0.12 (Fig. S3b). At the same time low terrestrial fetch (low radon concentration) was observed (Mallet et al., 2016). Moreover, the chlorides collected on filters were prominent during the period of oceanic influence (Fig. S3a). This suggests that a significant portion of chlorides detected on the BAM filters was of a sea salt origin, which is refractory and therefore not well measured by the AMS, thereby explaining the poor chloride correlation.

3.2 Biomass burning aerosols and aging

In general, BB-related particulate matter can be easily distinguished from other aerosol sources by chemical composition. Levoglucosan is a common molecular tracer of plume emissions (Simoneit et al., 1999) and has been extensively used as a BB chemical signature (Jordan et al., 2006;Simoneit, 2002). Moreover, the AMS ~~organic~~ OA signal intensity (fragment $C_2H_4O_2^+$) (Org 60) is directly correlated to the concentration of levoglucosan-like species (Alfarra et al., 2007;Simoneit et al., 1999) and can therefore be applied as a valuable BB marker. Fire sources also contribute to high potassium levels (Li et al., 2003). Figure 3 illustrates the time series of Org 60 obtained from the AMS and levoglucosan and soluble non-sea salt potassium sampled by the BAM. Prominent signals of these BB tracers were present during the observed close BB periods, which confirm that the source of the detected aerosols is BB.

In order to discriminate BB aerosol from other sources and estimate the degree of BB aerosol aging (processing), a graphical method introduced by Cubison et al. (2011) has been applied here (Fig. 4). The majority of data points (94 % of the dataset) had f60 values above the background limit of 0.003, indicated with black vertical dashed lines. Thus, the detected OA during SAFIRED can be attributed mostly to BB aerosol.

Chemical aging of BB-related OA typically leads to f60 depletion and increased f44 (Grieshop et al., 2009;Cubison et al., 2011;Ortega et al., 2013;Ng et al., 2010;Zhao et al., 2014;Capes et al., 2008;Jolleys et al., 2015). In general, this trend was observed in this study for distant fires, with the data trending towards the top left corner of the diagram (Fig. 4b). Apart from aerosol processing, changes in f44 and f60 can be attributed to burning conditions and/or materials. The variability observed in f44 vs. f60 for close BB events (Fig. 4a) can reflect BB plumes generated during different burning conditions but also different atmospheric processing of BB masses. One more factor that can influence the f44 vs f60 trend for both close and distant fire is mixing of the BB plume with air masses containing aerosol particles from other sources (dilution effect). On average distant BB plumes were characterized by lower fire tracer f60 compared to the close BB emissions. Furthermore, distant fire plumes indicated a higher portion of oxygenated compounds (i.e., higher f44 values), relative to close plumes. The maximum f44 value ranged between 0.20 and 0.23 in this study, which agrees well with previously observed f44 values for oxidized BB emissions in ambient measurements (Cubison et al., 2011). The f44 parameter increased to values characteristic of LV-OOA in the distant BB and yet f60 values were substantially above the background value of 0.003. This confirms that levoglucosan-like species carried by the BB plume did not degrade to background levels even as oxidized species were formed. Thus, f60 is a reasonable marker of distant BB in this study.

All data fall into the f44 vs. f43 triangular plot range for ambient data, introduced by Ng et al. (2010) (Fig. S4). Ng et al. (2010) observed that typical ambient OA data slopes from the bottom right to the top left of the f44 vs. f43 plot, and that this trend can be attributed to photochemical processing of ambient air masses. A similar pattern was observed in this study for the distant periods (Fig. S4b). A wide range in f44 can be attributed to different processed (aged) BB-related OA, but different burning material and/or conditions cannot be excluded. The observed evolution trend in f44 vs f43 for distant fires can be also influenced by mixing between the plumes. In contrast the f43 values for close BB (Fig. S4a) are located in a narrow f43 range from 0.05 to 0.08 and do not change considerably with increasing f44. This can be a result of insignificant atmospheric processing in the case of close fires. The wide range in f44 can be attributed to differences in burning conditions for close BB. ~~One more factor that can influence f44 vs f60 trend for both close and distant fire is dilution effect.~~

3.2.1 Ozone formation

The emissions from BB sources promote ozone production in the troposphere by increasing the concentrations of key ozone-forming precursors (NMOCs, NO_X and CO). Air mass photochemical activity can be estimated through the observation of changes in ozone concentration with aging, particularly the change in the $\Delta O_3/\Delta CO$ ratio, where ΔCO and ΔO_3 refer to enhancements above background concentrations. ΔCO accounts for dilution, as it is a relatively long lived atmospheric species. The minimum CO value of 80 ppb measured during June at the ATARS site was used as the background concentration level. Similarly a minimum ozone concentration of 10 ppb was considered to be the background level in these calculations. On average, the $\Delta O_3/\Delta CO$ ratio increases with f44 and decreases with f60, indicating increased photochemical processing of OA in plumes with atmospheric aging and ozone production (Fig. 4c and Fig. 4d).

$\Delta O_3/\Delta CO$ values vary between -0.1 and 0.9 which is within the observed range in other studies (Jaffe and Wigder, 2012). A negative ratio may indicate fresh BB emissions where ozone was removed by atmospheric reaction with nitric oxide (NO) emitted in high amounts from fire sources, as suggested by Yokelson et al. (2003). Close fire emissions were characterized by significantly lower ozone enrichments (average $\Delta O_3/\Delta CO$ of 0.15) compared to plumes detected from the distant BB emissions (average $\Delta O_3/\Delta CO$ of 0.31) which represent higher photochemical activity within more processed air masses. These values agree with observed $\Delta O_3/\Delta CO$ ratio values for plumes aged for less than 1-2 days (average $\Delta O_3/\Delta CO$ of 0.14) and for 2-5 days (average $\Delta O_3/\Delta CO$ of 0.35) in tropical/subtropical regions (Jaffe and Wigder, 2012). The $\Delta O_3/\Delta CO$ enrichments for close BB period indicate that aging of close emissions cannot be excluded. These significant ozone enrichments in BB plumes illustrate high NO_X and NMOC loadings emitted from fire sources and photochemically active air masses.

~~3.2.2 Secondary organic aerosol (SOA) formation~~

Since increased photochemical activity was identified in BB air masses, the change in $\Delta OA/\Delta CO$ ratio was investigated in order to determine whether additional OA was produced in the BB plumes (Fig. 4e and Fig. 4f). The lowest OA concentration observed during the campaign of 0.09 $\mu g\ m^{-3}$ was taken as a background value in these calculations. Figures show no particular trend in $\Delta OA/\Delta CO$ ratio with f44. The $\Delta OA/\Delta CO$ ratio remains quite constant despite increases in f44

(Fig. S5). ~~In addition, diurnal patterns of the f44, $\Delta O_3/\Delta CO$ and ΔOA/ΔCO ratios were investigated, for close and distant BB periods separately (Fig. 5a and Fig. 5b, respectively). The parameter f44 was used to indicate the level of oxygenation that can be caused by the photochemical changes and $\Delta O_3/\Delta CO$ as a parameter of photochemical activity. It must be noted that simply examining ΔOA/ΔCO vs time of day is a simplified approach which does not fully take into account the total photochemical history of the air mass. There was an increase in ΔOA/ΔCO ratio with an increase in f44 and $\Delta O_3/\Delta CO$ in the late morning and early afternoon for close and for distant BB periods. This is likely due to condensation of organics onto pre-existing particles. The decrease in the ΔOA/ΔCO ratio later in the afternoon could indicate OA loss due to fragmentation and subsequent evaporation from the particulate phase. As suggested by Kroll et al. (2009), OA loss can reflect dominance of the fragmentation pathways in the formation of more oxidized OA. Therefore it is suggested that increased photochemical activity of BB-influenced air masses, illustrated by increase in $\Delta O_3/\Delta CO$ and likely due to oxygenation of OA (f44 increase), was accompanied by an increase in ΔOA/ΔCO ratio, indicating SOA formation. Moreover, the decrease in ΔOA/ΔCO ratio later in the day can be a result of fragmentation and subsequent evaporation.~~

3.2.~~3~~ 2 f44-resolved size distribution

Atmospheric aging of plume particles increases particle diameter due to gas to particle transfer of organic and inorganic gaseous species (Martins et al., 1998). In order to estimate whether the aging of BB masses during SAFIRED influenced particle size, average SMPS size distributions and AMS size distributions for ~~organics~~OA, both categorised based on different f44 ranges, were examined (Fig. ~~6~~5). It is important to emphasise that the SMPS uses electrical mobility diameter, while the AMS uses vacuum aerodynamic diameter. The close and distant BB periods were analysed separately. The f44 values were classified into four groups that represent different aging stages (0.05<f44<0.1, 0.1<f44<0.15, 0.15<f44<0.2, 0.2<f44<0.25). The first f44 bin (0.05<f44<0.1) was not considered in case of the distant BB periods, as only a few data points were in this range (Fig. 4). The same was done for the highest f44 bin (0.2<f44<0.25) for close BB periods. According to the SMPS data, the average particle mode varied between 101 – 113 nm and 104 – 106 nm for close and distant BB periods, respectively. The average mode for ~~organics~~ OA showed larger sizes and varied between 259 – 293 nm and 293 – 305 nm for close and distant BB periods, respectively. Increased f44 was accompanied by a reduction in SMPS particle size for close plumes, going from 113 nm (0.05<f44<0.1) to 101 nm (0.1<f44<0.15). The same trend was observed for the ~~organic aerosols~~OA. Considering both AMS and SMPS data for distant fires, there was ~~no~~ little ~~considerable~~ change in diameter with aging from less aged to more aged BB air masses as ~~.~~ t~~T~~he particle modes show only slight differences between different f44 bins. ~~This is not consistent with the observed increase in OA for distant fires.~~ Changes in size distribution will be discussed further in the Sect. 3.2.~~4~~ 3 where results related to specific BB events are presented.

3.2.~~4~~ 3 Biomass burning events

Five single source BB events were analysed here (Fig. 2) in order to demonstrate the significant variability of fires detected during the SAFIRED. These episodes were within previously defined close BB periods. Mass spectra for selected ~~signatures~~

events and their time of detection are given in Fig. S6. The spectral signature is similar for these events, with prominent BB-related signals at m/z 60, 73, 29 and 39. However, a significant variation in m/z fragments, especially in m/z 44, can be observed. More detail about these BB events is given in Table 1 and discussed in the following paragraphs. Different factors were considered including f44, time of day, $\Delta O_3/\Delta CO$, f60, f60/f73, ~~organic~~ OA concentration, mode diameter and MCE.

~~On 30th of May at around 2pm three hot spots (two having confidence level of approximately 50% and one of 70%) were detected within 2km on the NE from the ATARS (Fig. S7a - Fig.S7d). These hot spots likely illustrated two fire events. On the same day and time, 11km on the SE from the sampling site, cluster of events was observed, including 4 hot spots with the confidence level between 94% and 100% and one of 78% confidence level. As all of them were spotted at the same time and within 1km distance, it is most likely that the one big fire has occurred. No other close events were observed over this time period. Cluster of hot spots was detected on the SE approximately 50km from the ATARS and big clusters at 100km and 150km, as well as on the SE. Moreover, 200km on E along the backtrajectories cluster of hot spots was observed.~~

On 30th of May, t~~T~~wo single source events, A and C, ~~were~~ have been identified and analysed here (Fig.2). ~~The e~~Event A illustrated ~~the~~ increased signal~~s~~ in the ~~afternoon~~ evening hours, when the wind was coming from the NE. ~~Therefore, the e~~Event A is likely the result of the hot spots detected within 2km from the ATARS to the NE (Fig. S7a and Fig. S7b). According to backtrajectories, air masses during these time period were ~~passing over the land affected by these fires and they were~~ transported from the fire events to ATARS within approximately 10 min. The average ~~organic~~ OA concentration was found to be 23 μg m^{-3}, with ~~the~~ concentrations going up to 45 μg m^{-3}. ~~High~~ For this event, a high average MCE value of 0.97 likely suggests flaming fire as the emission source and/or grass as a burning material (Desservettaz et al., 2016). Close to midnight the wind direction abruptly changed from NE to SE. At that time ~~The signal named as a C event~~ Event C was detected ~~over the night (Table 1). At that time wind direction was abruptly changed from the NE to SE. Therefore, the signal can be~~and was likely associated ~~to~~ with a cluster of fires 11 km to~~n~~ the SE (Fig. S7c and Fig. S7d). According to the backtrajectories, air masses took 20 min to reach~~ed~~ the ATARS ~~within 20 min~~ from the fire cluster. ~~Comparing~~ Compared to ~~the event~~ Event A, the average ~~organic~~ OA concentration for ~~the event~~ Event C was ~~more than threefold~~much higher with ~~the~~ a maximum value of approximately 130 μg m^{-3}. As the MCE was found to be similar (0.98) to E~~e~~vent A~~ value~~, ~~most likely~~ the higher signals most likely ~~illustrate~~ indicate a larger fire. The number of hot spots detected at~~on~~ the same time with high confidence level confirms this. Higher fire intensity can also be a reason for the higher f60 values for ~~the~~ E~~e~~vent C (0.027) compared to ~~event~~ Event A (0.016) (Table 1).

~~On 25th of June three hotspot clusters were observed close to ATARS (2km on E, 5km on NE and 10km on SE) (Fig. S7e-Fig. S7h). The cluster of hot spots observed 10 km from the sampling site had one of the highest hot spot's power (energy released by the fire) observed close to the ATARS (within 20 km) during the campaign (120 MW/km^2). Besides the close fires two big clusters around 60 km and 120 km on the SE from ATARS were detected on the same day.~~ On the 25th of June, two single-source events were observed and labelled as ~~events~~ Events F and G. Event F was related to a close fire (~~two hot spots of 60 and 100% confidence level,~~ within 2 km ~~on~~ to the E) whose emissions were clearly visible from ATARS (Fig. S7e and Fig. S7f). The detected plumes included a considerable portion of ~~oxygenated~~ OOA (average f44 value of 0.13, up to 0.18) that could be caused by high daytime photochemical activity. ~~The BB e~~Event F began at noon and ended at approximately 5 pm, i.e., it occurred during the period of highest photochemical activity. The relatively high $\Delta O_3/\Delta CO$ ratio (0.13) was elevated relative to the other close BB events, which suggests additional photochemical activity in the plume. This value falls into the range for fire emissions aged less than 1-2 days in tropical/subtropical regions (Jaffe and Wigder, 2012). However, the f44 value was highly variable during ~~the event~~ Event F, ranging from 0.07 to 0.18. Other parameters including f60 and ~~organics~~ OA varied as well. ~~On~~ At that time, the wind direction significantly ~~varied~~ fluctuated between ~~140°~~ SE and ~~80°~~ E and likely influenced changes in detected air mass. One of the explanations can be alternating detection of a fresh plume and aged masses coming from the distant fires with the change in wind. The low correlation between f60 and f73 might also be an indicator for detection of different BB air masses (Fig. S8). Relatively low ~~organic~~ OA mass loading and f60 values may be due to highly variable wind direction and/or burned area rather than combustion conditions (MCE of 0.93), as higher ~~organics~~ OA are expected for this MCE value. In contrast, ~~event~~ Event G resulted in the highest ~~organic~~ OA mass loading measured at ATARS (PM$_1$ concentration of ~350 µg m^{-3}). Moreover, ~~the~~ its ~~highest~~ chloride concentration was ~~observed~~ the highest ~~over~~ of the whole campaign (53 µg m^{-3})~~was at the time of G event~~. The source of emissions was probably within 10 km ~~on~~ SE of the sampling site (Fig. S7g and Fig. S7h). ~~and t~~The fire magnitude was illustrated by a large burned area observed the following morning (Mallet et al., 2016) and high power of fire ~~observed~~ (120 MW/km^2, the highest value observed during the campaign). Backtrajectory~~ies~~ analysis indicated that less than half an hour was needed for the air mass to reach the ATARS. High fire intensity was accompanied with smouldering burning conditions (MCE of 0.90) that resulted in high ~~organic~~ OA loadings and ~~high~~ levoglucosan concentrations (high f60) (Table 1). A low OOA fraction, f44 and~~,~~ $\Delta O_3/\Delta CO$ value (0.01) indicated that the plume was likely not aged, which is to be expected due to the proximity and time of the event (started at 10 pm and finished at 4 am).

Intense signals, including high ~~organic~~ OA concentrations, were also detected on the 9th of June (Fig. S7i and Fig. S7j). ~~On that day cluster of hot spots (all with the confidence level higher than 70%) was detected 5 km from ATARS. Number of distant hot spots was detected between 100 km and 200 km, on the SE from the ATARS.~~ Mallet et al. (2016) suggested that possible sources of ~~this event~~ Event E might be close fires (within 5 km from ATARS), distant fires (between 100 km and 200 km from ATARS) or a combination of both. According to backtrajectories, less than 10 min was enough for air masses to cross the distance between the 5 km fire cluster and the research station. Values for f44 (0.08) and $\Delta O_3/\Delta CO$ (0.02) suggested detection of fresh emissions. Moreover, the high f60 value of 0.032 supported this, as distant fires are not likely to be characterized with such a high portion of levoglucosan-like species. However, the possibility of contribution from distant BB plumes cannot be excluded, especially when considering the particle size distribution during ~~event~~ Event E. ~~The~~ This ~~particle size~~ distribution had a mode of 146 nm, while ~~events~~ Events F and G showed smaller size distributions with modes of 98 and 88 nm, respectively (Table 1). However, different burning material and conditions could also contribute to the larger size distribution mode during ~~event~~ Event E.

In summary, the backtrajectory analysis showed that not more than half an hour was needed for the air masses to reach the ATARS from each area affected by close fire events. All sampled aerosols had f44 values lower than 0.1, which likely reflects fresher aerosol masses. Only aerosols emitted from Event F had higher f44 values, which can be a reflection of aerosol processing but also different factors, including mixing of masses due to the abrupt wind changes. The variation between fires and their burning material and conditions, can also be seen through a wide range of MCE values, from 0.9 to 0.98. ~~In general, diversity of BB plumes was illustrated through high variability in chemical signature (e.g. large range of f44, from 0.06 to 0.18) for five intense fire events.~~ Events were characterised with different f60/f73 ratios (varying between 1.2 and 2.5), ~~but~~ and there was no trend in the relationship ~~of~~ between f60/f73 ratio and burning material/conditions (MCE values) (Fig. S8). In general, the diversity of BB plumes was illustrated through high variability in chemical signature ~~(e.g. large range of f44, from 0.06 to 0.18)~~ as a product of different burning conditions/material for these five intense fire events.

3.3 Positive Matrix Factorization (PMF)

Initially PMF was performed to assist with analysis of the aging observations rather than to apportion sources, since the main source (BB) is already known. This approach was intended to estimate whether the ratios of the different factors, e.g., fresh BBOA, aged BBOA or OOA, exhibited relationships with the age of separate BB plumes. The diversity of the plumes (including close fire plumes with spectra presented in Fig. S6), however, made PMF analysis difficult. The thousands of fires that occurred during the SAFIRED campaign contributed to a wide range of OA composition that reflect different burning materials, conditions, processing in the atmosphere and mixed fresh and aged emissions. The ratio of m/z 43 and 44 differed between plumes (Fig. S11) and since the AMS mass spectra were dominated by these masses, the PMF analysis returned factors that corresponded to individual plumes, even when distant fires were separately examined. In addition, high residuals during BB events could not be reduced even with an unreasonably large number of factors (Fig. S9). The PMF diagnostic plots can be found in Sect. S3.

Instead PMF analysis was applied on “background” data in order to determine the contribution of BB emissions and SOA to regional ambient PM_1 outside of the time periods dominated by BB events. The background time periods were determined by examining the plot of f44 vs. f43 (Fig. S11). Cut-offs of 0.15 for m/z 43 and 0.4 for f44 were chosen to remove the influence of periods dominated by BB events which show up as individual lines in f43 vs. f44 space. The background time period was 22% of the whole data period.

PMF performed on the background OA showed significantly smaller residuals (Fig. S12) and resulted in three factors, including a biomass burning OA factor (BBOA), oxygenated OA (OOA) and a factor that represented isoprene-derived OA (Fig. ~~7~~6). A two-factor solution did not extract the biogenic isoprene-derived OA factor while a four-factor solution resulted in splitting of profiles (Fig. S13). The biomass burning factor, with distinct m/z 60 and 73 signals, contributed to 24 % of the background aerosol. BBOA was also characterized by fragments related to fresh hydrocarbon-like ~~organics~~OA, e.g., m/z 27, 29, 41, 43, 55, and 57, and by prominent OOA-related m/z 28 and 44 signals. The large f44 value (an average f44 of 0.09) (Fig. S4) may indicate either the presence of processed BB aerosol and/or fresh emissions that contain ~~oxygenated ~~OOA species possibly due to the burning conditions (Heringa et al., 2012;Weimer et al., 2008). A good correlation was observed between the BBOA factor and Org 60 and CO signals (Fig. ~~7d~~ 6d and Fig. ~~7e~~6e). An OOA profile with prominent m/z 28 and 44, similar to LV-OOA profiles observed in previous studies, was extracted. Its diurnal trend is marked by a broad daily peak which correlates with the maximum temperature and reflects intense daytime photochemical activity. The OOA dominance (contribution of 47 %) and high degree of oxygenation (an average f44 of 0.23) (Fig. S4) illustrate the significance of OOA for this area. The third PMF factor can be related to background biogenic SOA, and is discussed in more detail in the Sect. 3.3.1.

3.3.1 Isoprene-derived OA

Isoprene epoxydiols (IEPOX) are important gas-phase precursors for IEPOX-SOA and are products of isoprene oxidation, mostly in low-NO_X environments (Paulot et al., 2009). Recent studies have showed that PMF performed on AMS OA data can be used to determine the total IEPOX contribution to SOA (Robinson et al., 2011;Lin et al., 2011;Budisulistiorini et al., 2013;Hu et al., 2015;Xu et al., 2016). A similar distinct PMF-resolved factor has been extracted in this study. In order to consider other possible pathways in isoprene-derived OA formation (Schwantes et al., 2015), the PMF factor has been named as isoprene-derived OA (Xu et al., 2016;Pye et al.) The isoprene-derived OA mass spectrum can be clearly distinguished from BBOA and OOA by an enhanced m/z 82 signal (Fig. ~~7a~~6a). In the HR analysis of this dataset, $C_5H_6O^+$ is the most dominant peak that contributes to m/z 82 (Fig. S15) and has been confirmed to be a reliable tracer for isoprene-derived OA (Hu et al., 2015). There was a strong correlation observed between the isoprene-derived OA factor and Org 82 ($C_5H_6O^+$) (R of 0.90) (Fig. ~~7f~~6f). The isoprene-derived OA factor profile was also characterized with enhanced peaks at m/z 53, 43 and 44. An AMS spectrum with the same prominent peaks was reported by Allen et al. (2008) for the Darwin region in the Northern Territory. This was observed during the monsoon-break period during the wet season in February, when fires were not common, and clean air of biogenic origin was suggested as a source. Moreover, our spectrum is similar to isoprene-related OA spectra reported previously (Robinson et al., 2011;Lin et al., 2011;Budisulistiorini et al., 2013). The average isoprene concentration measured during the campaign was 0.49 ± 0.78 ppb. However, it should be emphasised that monoterpene-derived OA can also influence the background level of $C_5H_6O^+$ (Hu et al., 2015). The average monoterpenes concentration for this study was found to be 0.22 ± 0.41 ppb.

~~The main path for isoprene-derived OA formation is proposed to be acid-catalysed IEPOX uptake (Lin et al., 2011;Lambe et al., 2015). According to calculations for the composition depended collection efficiency, 22% of the aerosol were acidic. In order to estimate whether the acidity of the particles had an influence on isoprene- derived OA generation in ATARS, the~~

~~correlation between sulfate (taken as proxy of aerosol acidity) and the isoprene-derived OA factor was examined. The correlation between the factor and sulfate can be considered as weak (R of 0.3) (Fig. S18). However, two periods can be clearly distinguished from the graph: the period before 5th of June and the period after 15th of June. While there is no correlation between sulfate and the isoprene-derived OA factor for the first period, when plotting only data collected from 15th of June, correlation is found to be slightly higher than the correlation for all background data (R of 0.4).~~

The isoprene/furan concentrations at m/z 69 (PTR-MS) were treated as an isoprene contribution due to the dominance of isoprene signal compared to furan, according to the samples analysed by gas chromatography-mass spectrometry (Fig. S17). The furan contribution was more significant in BB plumes during the close BB period, as suggested previously (Warneke et al., 2011). As expected, the isoprene/furan gas-phase concentration measured by the PTR-MS increased from noon till the late afternoon (Fig. S16). According to diurnal patterns of PMF isoprene-derived OA, there is no considerable change in ~~isoprene-derived OA~~factor concentration from noon throughout the day. The isoprene-derived OA fraction is expected to increase during daytime hours in accordance with enhancements in isoprene and gas-phase IEPOX (Hu et al., 2015). However, the isoprene-derived OA factor was prominent during night and morning hours. This night-time enhancement might be due to transport of distant air masses, or partitioning of lower volatility species into the particle phase as the temperature drops and relative humidity increases, as suggested by~~Significant isoprene-derived OA factor enhancement during the night time might be due to partitioning of lower volatility species onto the particles when the temperature drops and relative humidity increases as suggested by~~ Budisulistiorini et al. (2013).~~,~~ In addition, the boundary layer height becomes lower during the night, increasing the concentration of gaseous compounds. This boundary layer reduction might induce low volatility OA partitioning, contributing to the increase in isoprene-derived OA.~~due to transport of distant air masses, or lower boundary layer height. During the night, the boundary level lowers which increases the concentration of gaseous compounds and can induce partitioning of gases onto the particles. Therefore, the lower night-time boundary layer might create conditions for low volatility isoprene-derived OA partitioning and an increase in isoprene-derived OA.~~

A plot of f44 (CO_2^+) vs. f82 ($C_5H_6O^+$) (Org CO_2^+/Org and Org $C_5H_6O^+$/Org from HR data analysis, respectively) (Fig. ~~8~~7) introduced by Hu et al. (2015) can be used to distinguish IEPOX-SOA from SOA originating from other sources, including isoprene-derived SOA that are generated from species other than IEPOX. This plot also indicates the degree of aging of the IEPOX-SOA. The general pattern of f44 increase with f82 decrease is observed. With aging, OA becomes more oxidized and the $C_5H_6O^+$ signature decreases. This can be due to oxidation processes or mixing with more aged aerosol masses.

A background value for f82 ($C_5H_6O^+$) in environments strongly influenced by BB was suggested to be 0.0017 ~~and is indicated by the vertical dashed black line~~ (Hu et al., 2015). Looking at our data plotted in f44 vs. f82 a similar observation can be made (the vertical dashed black line indicates the f82 background of 0.0017). All data points are positioned above 0.0016 of f82 with an average value of 0.0061 ± 0.0036. The isoprene-derived OA factor average values for this campaign and two other ambient studies are marked in the plot. The f82 value for isoprene-derived OA factor observed here is similar to the reported f82 value for an urban site (Budisulistiorini et al., 2013), but lower compared to the factor observed for the Borneo forest (Robinson et al., 2011). The lower value for SAFIRED compared to the Borneo forest, considering that biogenic influence is significant for both environments, can be attributed to the high influence of BB emissions but also to the other SOA generated from different sources that prevail in the two regions.

As the most abundant NMOC, isoprene is a significant contributor to the global SOA budget (Guenther et al., 2012;Hallquist et al., 2009;Paulot et al., 2009). Isoprene-derived OA during the SAFIRED campaign accounted for 28 % of the total background OA which is similar to previous observations where the isoprene-derived OA fraction contribution varied from 6-36 %, depending on the environment (Hu et al., 2015). This confirms the importance of isoprene-derived OA for the Northern Territory environment even in times of high BB influence.

4. Conclusions

A one month long campaign called SAFIRED was conducted in northern Australia during a period of significant burning (early dry season). There was a significant influence of BB plumes on the atmospheric chemical profile at the time of campaign, reflected by high concentrations of gaseous and particle species including CO and PM$_1$ ~~organics~~OA, reaching maxima of ~10^4 ppb and 350 µg m^{-3} respectively during heavy BB episodes. Emitted aerosols were predominantly ~~organic~~ OA species (90 %) with a wide range of levels of oxidation. There was a clear overall increase of the highly oxygenated OA fraction and degradation of BB-related signatures with OA processing. This was shown by an overall trend of f44 increase and f60 decrease for distant fires. Plume emissions formed over the month period were photochemically active resulting in the production of tropospheric ozone. Close fire emissions were characterized by lower ozone enrichments (average $\Delta O_3/\Delta CO$ of 0.15) than plumes detected from the distant BB sources (average $\Delta O_3/\Delta CO$ of 0.31) which illustrate higher photochemical activity with more processed air masses. This emphasizes air mass ability for photochemical processing and production of SOA. ~~An increase in the ΔOA/ΔCO ratio with increase of f44 also suggests SOA formation.~~ According to these results, the OA oxidation level did not significantly influence particle size distributions. Diversity in BB emissions was illustrated through investigation of ~~five~~ selected fire events. Even across these five events, ~~The~~ the chemical signature varied significantly ~~for different fire events~~ (e.g. wide range in f44, from 0.06 to 0.18) which emphasises the need for a more comprehensive dataset that characterises the factors associated with burning material, conditions and processing.

PMF was employed to estimate BB influence on and SOA portion of background regional aerosol. A significant portion of ~~oxygenated~~ OOA (47 %), identified through high f44 (majority of data points between 0.1 and 0.25), and a significant portion of aged BBOA (~~47 and~~ 24 %~~, respectively~~) were observed. ~~The~~ This ~~latter~~ suggests considerable processing of aerosol in the atmosphere for this area. The remaining OA was attributed to the isoprene-derived OA factor (28 %), identified here for the first time in Australia. The OA mass spectrum with isoprene-derived OA characteristics previously reported in the wet season and now observed with prominent BB influence during the dry period, suggests the importance of biogenic isoprene sources for the Northern Territory area at all times of the year.

Observed photochemical activity of air masses ~~and enhancement of OA~~ with aging illustrates the importance of aging and likely SOA formation in the Northern Territory during the dry early season. SOA is recognized as a significant contributor to climate, environment and adverse human health effects. This study is an important step in addressing suggested further research related to tropical biomass burns and biogenic-related SOA in Australia (Rotstayn et al., 2009). As SOA yields are considerably underestimated and its formation is still not sufficiently understood, this study can facilitate understanding of SOA formation for Northern Territory savannah areas and also for the tropics in general. Additional measurements during late dry season (September-October) are needed as more intense and frequent fires occur during this period (Andersen et al., 2005;Williams et al., 1998). Moreover, the late dry season is suggested to have more aged emissions (Ristovski et al., 2010;Wardoyo et al., 2007). Therefore it is important to characterize SOA formation, and yield during this period.

Data availability. The underlying research data can be accessed upon request to the corresponding author (Branka Miljevic; b.miljevic@qut.edu.au).

Author contributions. Andelija Milic analysed and interpreted the data and prepared the manuscript. Marc Mallet operated the cToF-AMS and contributed to data analysis, interpretation and writing. Branka Miljevic installed the cToF-AMS, contributed to data analysis, interpretation and writing and supervised the work of Andelija Milic. Luke Cravigan set up the SMPS and contributed to data interpretation. Joel Alroe assisted in organizing the QUT instrumentation, data interpretation and writing the manuscript. Zoran Ristovski contributed to campaign organization and data interpretation and supervised the work of Andelija Milic. Leah Williams contributed to setting up the cToF-AMS, preliminary data analysis and data interpretation. Melita Keywood organized and led the campaign. Paul Selleck operated the BAM, analysed the data and contributed to data interpretation. Sarah Lawson operated the PTR-MS and analysed the data. James Ward operated the Ozone analyser and analysed the data. Maximilian Desservettaz operated the FTIR and SMPS and analysed the data. Clare Paton-Walsh contributed to campaign organization and running the campaign. All authors declare that they have no conflict of interest.

Acknowledgements. The authors thank Manjula Canagaratna for valuable discussions about interpreting the PMF analysis. The authors thank Min Cheng for providing the gas chromatography-mass spectrometry data. This work was supported by the Australian Research Council Discovery grant (DP120100126).

References

Aiken, A. C., DeCarlo, P. F., and Jimenez, J. L.: Elemental analysis of organic species with electron ionization high-resolution mass spectrometry, Analytical Chemistry, 79, 8350-8358, 2007.

Aiken, A. C., DeCarlo, P. F., Kroll, J. H., Worsnop, D. R., Huffman, J. A., Docherty, K. S., Ulbrich, I. M., Mohr, C., Kimmel, J. R., Sueper, D., Sun, Y., Zhang, Q., Trimborn, A., Northway, M. J., Ziemann, P. J., Canagaratna, M., Onasch, T., Alfarra, M. R., Prevot, A. S., Dommen, J., Duplissy, J., Metzger, A., Baltensperger, U., and Jimenez, J.: O/C and OM/OC ratios of primary, secondary, and ambient organic aerosols with high-resolution time-of-flight aerosol mass spectrometry, Environmental Science & Technology, 42, 4478-4485, 2008.

Akagi, S., Craven, J., Taylor, J., McMeeking, G., Yokelson, R., Burling, I., Urbanski, S., Wold, C., Seinfeld, J., Coe, H., Alvarado, M., and Weise, D.: Evolution of trace gases and particles emitted by a chaparral fire in California, Atmospheric Chemistry and Physics, 12, 1397-1421, 2012.

Alfarra, M. R., Prevot, A. S., Szidat, S., Sandradewi, J., Weimer, S., Lanz, V. A., Schreiber, D., Mohr, M., and Baltensperger, U.: Identification of the mass spectral signature of organic aerosols from wood burning emissions, Environmental science & technology, 41, 5770-5777, 2007.

Allen, G., Vaughan, G., Bower, K., Williams, P., Crosier, J., Flynn, M., Connolly, P., Hamilton, J., Lee, J., Saxton, J., Watson, N., Gallagher, M., Coe, H., Allan, J., Choularton, T., and Lewis, A.: Aerosol and trace-gas measurements in the Darwin area during the wet season, Journal of Geophysical Research: Atmospheres (1984–2012), 113, 2008.

Andersen, A. N., Cook, G. D., Corbett, L. K., Douglas, M. M., Eager, R. W., Russell-Smith, J., Setterfield, S. A., Williams, R. J., and Woinarski, J. C.: Fire frequency and biodiversity conservation in Australian tropical savannas: implications from the Kapalga fire experiment, Austral Ecology, 30, 155-167, 2005.

Bond, T. C., Streets, D. G., Yarber, K. F., Nelson, S. M., Woo, J. H., and Klimont, Z.: A technology-based global inventory of black and organic carbon emissions from combustion, Journal of Geophysical Research: Atmospheres (1984–2012), 109, 2004.

Bougiatioti, A., Stavroulas, I., Kostenidou, E., Zarmpas, P., Theodosi, C., Kouvarakis, G., Canonaco, F., Prévôt, A., Nenes, A., Pandis, S., and Mihalopoulos, N.: Processing of biomass-burning aerosol in the eastern Mediterranean during summertime, Atmospheric Chemistry and Physics, 14, 4793-4807, 2014.

Bouya, Z., Box, G. P., and Box, M. A.: Seasonal variability of aerosol optical properties in Darwin, Australia, Journal of Atmospheric and Solar-Terrestrial Physics, 72, 726-739, 2010.

Bowman, D. M., Dingle, J. K., Johnston, F. H., Parry, D., and Foley, M.: Seasonal patterns in biomass smoke pollution and the mid 20th-century transition from Aboriginal to European fire management in northern Australia, Global Ecology and Biogeography, 16, 246-256, 2007.

Brito, J., Rizzo, L., Morgan, W., Coe, H., Johnson, B., Haywood, J., Longo, K., Freitas, S., Andreae, M., and Artaxo, P.: Ground-based aerosol characterization during the South American Biomass Burning Analysis (SAMBBA) field experiment, Atmospheric Chemistry and Physics, 14, 12069-12083, 2014.

Budisulistiorini, S. H., Canagaratna, M. R., Croteau, P. L., Marth, W. J., Baumann, K., Edgerton, E. S., Shaw, S. L., Knipping, E. M., Worsnop, D. R., and Jayne, J. T.: Real-time continuous characterization of secondary organic aerosol derived from isoprene epoxydiols in downtown Atlanta, Georgia, using the Aerodyne Aerosol Chemical Speciation Monitor, Environmental science & technology, 47, 5686-5694, 2013.

Capes, G., Johnson, B., McFiggans, G., Williams, P., Haywood, J., and Coe, H.: Aging of biomass burning aerosols over West Africa: Aircraft measurements of chemical composition, microphysical properties, and emission ratios, Journal of Geophysical Research: Atmospheres (1984–2012), 113, 2008.

Carr, S. B., Gras, J., Hackett, M., and Keywood, M.: Aerosol Characteristics in the Northern Territory of Australia During the Dry Season With an Emphasis on Biomass Burning, DTIC Document, 2005.

Chow, J. C., Watson, J. G., Chen, L.-W. A., Chang, M. O., Robinson, N. F., Trimble, D., and Kohl, S.: The IMPROVE_A temperature protocol for thermal/optical carbon analysis: maintaining consistency with a long-term database, Journal of the Air & Waste Management Association, 57, 1014-1023, 2007.

Crutzen, P. J., and Andreae, M. O.: Biomass burning in the tropics: Impact on atmospheric chemistry and biogeochemical cycles, Science, 250, 1669-1678, 1990.

Cubison, M., Ortega, A., Hayes, P., Farmer, D., Day, D., Lechner, M., Brune, W., Apel, E., Diskin, G., and Fisher, J.: Effects of aging on organic aerosol from open biomass burning smoke in aircraft and laboratory studies, Atmospheric Chemistry and Physics, 11, 12049-12064, 2011.

DeCarlo, P., Dunlea, E., Kimmel, J., Aiken, A., Sueper, D., Crounse, J., Wennberg, P., Emmons, L., Shinozuka, Y., and Clarke, A.: Fast airborne aerosol size and chemistry measurements above Mexico City and Central Mexico during the MILAGRO campaign, Atmos. Chem. Phys, 8, 4027-4048, 2008.

DeCarlo, P., Ulbrich, I., Crounse, J., Foy, B. d., Dunlea, E., Aiken, A., Knapp, D., Weinheimer, A., Campos, T., Wennberg, P., and Jimenez, J.: Investigation of the sources and processing of organic aerosol over the Central Mexican Plateau from aircraft measurements during MILAGRO, Atmospheric Chemistry and Physics, 10, 5257-5280, 2010.

Desservettaz, M., Paton-Walsh, C., Griffith, D., Kettlewell, G., Keywood, M., Schoot, M. V., JasonWard, Mallet, M., Ristovski, Z., Miljevic, B., Milic, A., Howard, D., Edwards, G., and Atkinson, B.: Emission factors of trace gases and particles from tropical savanna fires in Australia, submitted to Journal of Geophysical Research 2016.

Edwards, D., Pétron, G., Novelli, P., Emmons, L., Gille, J., and Drummond, J.: Southern Hemisphere carbon monoxide interannual variability observed by Terra/Measurement of Pollution in the Troposphere (MOPITT), Journal of Geophysical Research: Atmospheres, 111, 2006.

Formenti, P., Elbert, W., Maenhaut, W., Haywood, J., Osborne, S., and Andreae, M.: Inorganic and carbonaceous aerosols during the Southern African Regional Science Initiative (SAFARI 2000) experiment: Chemical characteristics, physical properties, and emission data for smoke from African biomass burning, Journal of Geophysical Research: Atmospheres (1984–2012), 108, 2003.

Grieshop, A., Logue, J., Donahue, N., and Robinson, A.: Laboratory investigation of photochemical oxidation of organic aerosol from wood fires 1: measurement and simulation of organic aerosol evolution, Atmospheric Chemistry and Physics, 9, 1263-1277, 2009.

Griffith, D., Deutscher, N., Caldow, C., Kettlewell, G., Riggenbach, M., and Hammer, S.: A Fourier transform infrared trace gas and isotope analyser for atmospheric applications, Atmospheric Measurement Techniques, 5, 2481-2498, 2012.

Griffith, D. W.: Synthetic calibration and quantitative analysis of gas-phase FT-IR spectra, Applied spectroscopy, 50, 59-70, 1996.

Guenther, A., Jiang, X., Heald, C., Sakulyanontvittaya, T., Duhl, T., Emmons, L., and Wang, X.: The Model of Emissions of Gases and Aerosols from Nature version 2.1 (MEGAN2. 1): an extended and updated framework for modeling biogenic emissions, 2012.

Guenther, C.: Estimates of global terrestrial isoprene emissions using MEGAN (Model of Emissions of Gases and Aerosols from Nature), Atmospheric Chemistry and Physics, 6, 2006.

Hallquist, M., Wenger, J., Baltensperger, U., Rudich, Y., Simpson, D., Claeys, M., Dommen, J., Donahue, N., George, C., Goldstein, A., Hamilton, J., Herrmann, H., Hoffmann, D., Iinuma, Y., Jang, M., Jenkin, M., Jimenez, J., Keindler-Scharr, A., Maenhaut, W., McFiggans, G., Mentel, T., Monod, A., Prevot, A., Seinfeld, J., Surratt, J., Szmigielski, R., and Wildt, J.: The formation, properties and impact of secondary organic aerosol: current and emerging issues, Atmos. Chem. Phys, 9, 5155-5236, 2009.

Haywood, J., and Boucher, O.: Estimates of the direct and indirect radiative forcing due to tropospheric aerosols: A review, Reviews of geophysics, 38, 513-543, 2000.

He, C., Murray, F., and Lyons, T.: Monoterpene and isoprene emissions from 15 Eucalyptus species in Australia, Atmospheric Environment, 34, 645-655, 2000.

Heringa, M., DeCarlo, P., Chirico, R., Tritscher, T., Dommen, J., Weingartner, E., Richter, R., Wehrle, G., Prévôt, A., and Baltensperger, U.: Investigations of primary and secondary particulate matter of different wood combustion appliances with a high-resolution time-of-flight aerosol mass spectrometer, Atmos. Chem. Phys, 11, 5945-5957, 2011.

Heringa, M., DeCarlo, P., Chirico, R., Lauber, A., Doberer, A., Good, J., Nussbaumer, T., Keller, A., Burtscher, H., and Richard, A.: Time-resolved characterization of primary emissions from residential wood combustion appliances, Environmental science & technology, 46, 11418-11425, 2012.

Hobbs, P. V., Sinha, P., Yokelson, R. J., Christian, T. J., Blake, D. R., Gao, S., Kirchstetter, T. W., Novakov, T., and Pilewskie, P.: Evolution of gases and particles from a savanna fire in South Africa, Journal of Geophysical Research: Atmospheres (1984–2012), 108, 2003.

Hu, W., Campuzano-Jost, P., Palm, B., Day, D., Ortega, A., Hayes, P., Krechmer, J., Chen, Q., Kuwata, M., Liu, Y., McKinney, K., Martin, S. T., Hu, M., Budisulistiorini, S. H., Riva, M., Surratt, J., Clair, J. M. S., Isaacman, G., Yee, L., Goldstein, A., Carbone, S., Brito, J., Artaxo, P., De Gouw, J., Koss, A., Wisthaler, A., Mikoviny, T., Karl, T., Kaser, L., Jud, W., Hansel, A., Docherty, K., Alexander, M., Robinson, A., Coe, H., Allan, J., Canagaratna, M., Paulot, F., and Jimenez, J.:

Characterization of a real-time tracer for isoprene epoxydiols-derived secondary organic aerosol (IEPOX-SOA) from aerosol mass spectrometer measurements, Atmospheric Chemistry and Physics, 15, 11807-11833, 2015.

Hurst, D. F., Griffith, D. W., and Cook, G. D.: Trace gas emissions from biomass burning in tropical Australian savannas, Journal of Geophysical Research: Atmospheres, 99, 16441-16456, 1994.

Jaffe, D. A., and Wigder, N. L.: Ozone production from wildfires: A critical review, Atmospheric Environment, 51, 1-10, 2012.

Jimenez, J., Canagaratna, M., Donahue, N., Prevot, A., Zhang, Q., Kroll, J. H., DeCarlo, P. F., Allan, J. D., Coe, H., Ng, N., Aiken, A., Docherty, K., Ulbrich, I., Grieshop, A. P., Robinson, A., Duplissy, J., Smith, J. D., Wilson, K. R., Lanz, V., Hueglin, C., Sun, J., Tian, J., Laaksonen, A., Raatikainen, T., Rautiainen, J., Vaattovaara, P., Ehn, M., Kulmala, M., Tomlinson, J., Collins, D., Cubison, M. J., Dunlea, E., Huffman, J. A., Onasch, T., Alfarra, M. R., Williams, P., Bower, K. N., Kondo, Y., Schneider, J., Drewnick, F., Borrmann, S., Weimer, S., Demerjian, K. L., Salcedo, D., Cottrell, L., Griffin, R., Takami, A., Miyoshi, T., Hatakeyama, S., Shimono, A., Sun, J., Zhang, J., Dzepina, K., Kimmel, J. R., Sueper, D., Jayne, J. T., Herndon, S., Trimborn, A., Williams, L. R., Wood, E., Middlebrook, A., Kolb, C. E., Baltensperger, U., and Worsnop, D. R.: Evolution of organic aerosols in the atmosphere, Science, 326, 1525-1529, 2009.

Jolleys, M., Coe, H., McFiggans, G., Taylor, J., O'Shea, S., Le Breton, M., Bauguitte, S.-B., Moller, S., Di Carlo, P., and Aruffo, E.: Properties and evolution of biomass burning organic aerosol from Canadian boreal forest fires, Atmospheric Chemistry and Physics, 15, 3077-3095, 2015.

Jordan, T. B., Seen, A. J., and Jacobsen, G. E.: Levoglucosan as an atmospheric tracer for woodsmoke, Atmospheric Environment, 40, 5316-5321, 2006.

Kleinman, L. I., Springston, S. R., Daum, P. H., Lee, Y.-N., Nunnermacker, L., Senum, G., Wang, J., Weinstein-Lloyd, J., Alexander, M., Hubbe, J., Ortega, A., Canagaratna, M., and Jayne, J. T.: The time evolution of aerosol composition over the Mexico City plateau, Atmospheric Chemistry and Physics, 8, 1559-1575, 2008.

Kroll, J. H., Smith, J. D., Che, D. L., Kessler, S. H., Worsnop, D. R., and Wilson, K. R.: Measurement of fragmentation and functionalization pathways in the heterogeneous oxidation of oxidized organic aerosol, Physical Chemistry Chemical Physics, 11, 8005-8014, 2009.

Lacey, C., Walker, J., and Noble, I.: Fire in Australian tropical savannas, in: Ecology of tropical savannas, Springer, 246-272, 1982.

Lambe, A., Chhabra, P., Onasch, T., Brune, W., Hunter, J., Kroll, J., Cummings, M., Brogan, J., Parmar, Y., and Worsnop, D.: Effect of oxidant concentration, exposure time, and seed particles on secondary organic aerosol chemical composition and yield, Atmospheric Chemistry and Physics, 15, 3063-3075, 2015.

Lanz, V., Alfarra, M., Baltensperger, U., Buchmann, B., Hueglin, C., and Prévôt, A.: Source apportionment of submicron organic aerosols at an urban site by factor analytical modelling of aerosol mass spectra, Atmospheric Chemistry and Physics, 7, 1503-1522, 2007.

Li, J., Pósfai, M., Hobbs, P. V., and Buseck, P. R.: Individual aerosol particles from biomass burning in southern Africa: 2, Compositions and aging of inorganic particles, Journal of Geophysical Research: Atmospheres, 108, 2003.

Li, W., Shao, L., and Buseck, P.: Haze types in Beijing and the influence of agricultural biomass burning, Atmospheric Chemistry and Physics, 10, 8119-8130, 2010.

Lin, Y.-H., Zhang, Z., Docherty, K. S., Zhang, H., Budisulistiorini, S. H., Rubitschun, C. L., Shaw, S. L., Knipping, E. M., Edgerton, E. S., Kleindienst, T. E., Gold, A., and Surratt, J.: Isoprene epoxydiols as precursors to secondary organic aerosol formation: acid-catalyzed reactive uptake studies with authentic compounds, Environmental science & technology, 46, 250-258, 2011.

Liu, X., Van Espen, P., Adams, F., Cafmeyer, J., and Maenhaut, W.: Biomass burning in southern Africa: Individual particle characterization of atmospheric aerosols and savanna fire samples, Journal of Atmospheric Chemistry, 36, 135-155, 2000.

Mallet, M. D., Desservettaz, M. J., Miljevic, B., Milic, A., Ristovski, Z. D., Alroe, J., Cravigan, L. T., Jayaratne, E. R., Paton-Walsh, C., Griffith, D. W. T., Wilson, S. R., Kettlewell, G., Vanderschoot, M. V., Selleck, P., Reisen, F., Lawson, S. J., Ward, J., Harnwell, J., Cheng, M., Gillett, R. W., Molloy, S. B., Howard, D., Nelson, P. F., Morrison, A. L., Edwards, G. C., Williams, A. G., Chambers, S. D., Werczynski, S., Williams, L. R., Winton, V. H. L., Atkinson, B., Wang, X., and Keywood, M. D.: Biomass burning emissions in north Australia during the early dry season: an overview of the 2014 SAFIRED campaign, Phys. Discuss., doi:10.5194/acp-2016-866, in review, 2016.

Martins, J. V., Dunlap, M. R., and Liousse, C.: Physical, chemical, and optical properties of regional hazes dominated by smoke in Brazil, Journal of Geophysical Research, 103, 32,059-032,080, 1998.

Middlebrook, A. M., Bahreini, R., Jimenez, J. L., and Canagaratna, M. R.: Evaluation of composition-dependent collection efficiencies for the aerodyne aerosol mass spectrometer using field data, Aerosol Science and Technology, 46, 258-271, 2012.

Mitchell, R., Forgan, B., Campbell, S., and Qin, Y.: The climatology of Australian tropical aerosol: evidence for regional correlation, Geophysical Research Letters, 40, 2384-2389, 2013.

Ng, N., Canagaratna, M., Zhang, Q., Jimenez, J., Tian, J., Ulbrich, I., Kroll, J., Docherty, K., Chhabra, P., Bahreini, R., Murphy, S., Seinfeld, J., Hildebrandt Ruiz, L., Donahue, N. M., DeCarlo, P., Lanz, V., Prevot, A., Dinar, E., Rudich, Y., and Worsnop, D. R.: Organic aerosol components observed in Northern Hemispheric datasets from Aerosol Mass Spectrometry, Atmospheric Chemistry and Physics, 10, 4625-4641, 2010.

O'Brien, D., and Mitchell, R.: Atmospheric heating due to carbonaceous aerosol in northern Australia—confidence limits based on TOMS aerosol index and sun-photometer data, Atmospheric Research, 66, 21-41, 2003.

Ortega, A., Day, D., Cubison, M., Brune, W., Bon, D., de Gouw, J., and Jimenez, J.: Secondary organic aerosol formation and primary organic aerosol oxidation from biomass-burning smoke in a flow reactor during FLAME-3, Atmospheric Chemistry and Physics, 13, 11551-11571, 2013.

Paatero, P., and Tapper, U.: Positive matrix factorization: A non-negative factor model with optimal utilization of error estimates of data values, Environmetrics, 5, 111-126, 1994.

Paatero, P.: The multilinear engine—a table-driven, least squares program for solving multilinear problems, including the n-way parallel factor analysis model, Journal of Computational and Graphical Statistics, 8, 854-888, 1999.

Paatero, P., and Hopke, P. K.: Rotational tools for factor analytic models, Journal of Chemometrics, 23, 91-100, 2009.

Parrington, M., Palmer, P., Lewis, A., Lee, J., Rickard, A., Carlo, P. D., Taylor, J., Hopkins, J., Punjabi, S., Oram, D., Forster, G., Aruffo, E., Moller, S., Bauguitte, S.-B., Allan, J., Coe, H., and Leigh, R.: Ozone photochemistry in boreal biomass burning plumes, Atmospheric Chemistry and Physics, 13, 7321-7341, 2013.

Paulot, F., Crounse, J. D., Kjaergaard, H. G., Kürten, A., Clair, J. M. S., Seinfeld, J. H., and Wennberg, P. O.: Unexpected epoxide formation in the gas-phase photooxidation of isoprene, Science, 325, 730-733, 2009.

Penner, J., Chuang, C., and Grant, K.: Climate forcing by carbonaceous and sulfate aerosols, Clim. Dynamm., 14, 839–851, ISI, 1998.

Pye, H. O., Murphy, B. N., Xu, L., Ng, N. L., Carlton, A. G., Guo, H., Weber, R., Vasilakos, P., Appel, K. W., and Budisulistiorini, S. H.: On the implications of aerosol liquid water and phase separation for organic aerosol mass,

Real, E., Law, K., Weinzierl, B., Fiebig, M., Petzold, A., Wild, O., Methven, J., Arnold, S., Stohl, A., Huntrieser, H., Roiger, A., Schlager, H., Stewart, D., Avery, M., Sachse, G. W., Browell, E., Ferrare, R., and Blake, D. R.: Processes influencing ozone levels in Alaskan forest fire plumes during long-range transport over the North Atlantic, Journal of Geophysical Research: Atmospheres (1984–2012), 112, 2007.

Reid, J., Koppmann, R., Eck, T., and Eleuterio, D.: A review of biomass burning emissions part II: intensive physical properties of biomass burning particles, Atmospheric Chemistry and Physics, 5, 799-825, 2005.

Ristovski, Z. D., Wardoyo, A. Y., Morawska, L., Jamriska, M., Carr, S., and Johnson, G.: Biomass burning influenced particle characteristics in Northern Territory Australia based on airborne measurements, Atmospheric Research, 96, 103-109, 2010.

Roberts, G. C., Artaxo, P., Zhou, J., Swietlicki, E., and Andreae, M. O.: Sensitivity of CCN spectra on chemical and physical properties of aerosol: A case study from the Amazon Basin, Journal of Geophysical Research: Atmospheres (1984–2012), 107, LBA 37-31-LBA 37-18, 2002.

Robinson, N., Hamilton, J., Allan, J., Langford, B., Oram, D., Chen, Q., Docherty, K., Farmer, D., Jimenez, J., and Ward, M.: Evidence for a significant proportion of Secondary Organic Aerosol from isoprene above a maritime tropical forest, Atmospheric Chemistry and Physics, 11, 1039-1050, 2011.

Rotstayn, L. D., Keywood, M. D., Forgan, B. W., Gabric, A. J., Galbally, I. E., Gras, J. L., Luhar, A. K., McTainsh, G. H., Mitchell, R. M., and Young, S. A.: Possible impacts of anthropogenic and natural aerosols on Australian climate: a review, International Journal of Climatology, 29, 461-479, 2009.

Russell-Smith, J., Yates, C. P., Whitehead, P. J., Smith, R., Craig, R., Allan, G. E., Thackway, R., Frakes, I., Cridland, S., Meyer, M. C., and Gill, A.: Bushfires' down under': patterns and implications of contemporary Australian landscape burning, International Journal of Wildland Fire, 16, 361-377, 2007.

Schwantes, R. H., Teng, A. P., Nguyen, T. B., Coggon, M. M., Crounse, J. D., St. Clair, J. M., Zhang, X., Schilling, K. A., Seinfeld, J. H., and Wennberg, P. O.: Isoprene NO3 Oxidation Products from the RO2+ HO2 Pathway, The Journal of Physical Chemistry A, 119, 10158-10171, 2015.

Simoneit, B. R., Schauer, J. J., Nolte, C., Oros, D. R., Elias, V. O., Fraser, M., Rogge, W., and Cass, G. R.: Levoglucosan, a tracer for cellulose in biomass burning and atmospheric particles, Atmospheric Environment, 33, 173-182, 1999.

Simoneit, B. R.: Biomass burning—a review of organic tracers for smoke from incomplete combustion, Applied Geochemistry, 17, 129-162, 2002.

Ulbrich, I., Canagaratna, M., Zhang, Q., Worsnop, D., and Jimenez, J.: Interpretation of organic components from Positive Matrix Factorization of aerosol mass spectrometric data, Atmospheric Chemistry and Physics, 9, 2891-2918, 2009.

Wang, C., and Prinn, R. G.: Impact of emissions, chemistry and climate on atmospheric carbon monoxide: 100-yr predictions from a global chemistry–climate model, Chemosphere-Global Change Science, 1, 73-81, 1999.

Ward, D., and Radke, L.: Emissions measurements from vegetation fires: A comparative evaluation of methods and results, 1993.

Wardoyo, A. Y., Morawska, L., Ristovski, Z. D., Jamriska, M., Carr, S., and Johnson, G.: Size distribution of particles emitted from grass fires in the Northern Territory, Australia, Atmospheric Environment, 41, 8609-8619, 2007.

Warneke, C., Roberts, J., Veres, P., Gilman, J., Kuster, W., Burling, I., Yokelson, R., and de Gouw, J.: VOC identification and inter-comparison from laboratory biomass burning using PTR-MS and PIT-MS, International Journal of Mass Spectrometry, 303, 6-14, 2011.

Weimer, S., Alfarra, M., Schreiber, D., Mohr, M., Prévôt, A., and Baltensperger, U.: Organic aerosol mass spectral signatures from wood-burning emissions: Influence of burning conditions and wood type, Journal of Geophysical Research: Atmospheres (1984–2012), 113, 2008.

Williams, R., Gill, A., and Moore, P.: Seasonal changes in fire behaviour in a tropical savanna in northern Australia, International Journal of Wildland Fire, 8, 227-239, 1998.

Xu, L., Middlebrook, A. M., Liao, J., Gouw, J. A., Guo, H., Weber, R. J., Nenes, A., Lopez-Hilfiker, F. D., Lee, B. H., and Thornton, J. A.: Enhanced formation of isoprene-derived organic aerosol in sulfur-rich power plant plumes during Southeast Nexus, Journal of Geophysical Research: Atmospheres, 121, 2016.

Yokelson, R. J., Bertschi, I. T., Christian, T. J., Hobbs, P. V., Ward, D. E., and Hao, W. M.: Trace gas measurements in nascent, aged, and cloud-processed smoke from African savanna fires by airborne Fourier transform infrared spectroscopy (AFTIR), Journal of Geophysical Research: Atmospheres (1984–2012), 108, 2003.

Yokelson, R. J., Crounse, J., DeCarlo, P., Karl, T., Urbanski, S., Atlas, E., Campos, T., Shinozuka, Y., Kapustin, V., Clarke, A., Weinheimer, A., Knapp, D., Montzga, L., Holloway, J., Weibring, P., Flocke, F., Zheng, W., Toohey, D., Wennberg, P. O., Wiedinmyer, C., Mauldin, R. L., Fried, A., Richter, D., Walega, J., Jimenez, J., Adachi, K., Buseck, P. R., Hall, S., and Shetter, R.: Emissions from biomass burning in the Yucatan, Atmospheric Chemistry and Physics, 9, 5785-5812, 2009.

Zhang, Q., Jimenez, J., Canagaratna, M., Allan, J., Coe, H., Ulbrich, I., Alfarra, M., Takami, A., Middlebrook, A., Sun, Y., Dzepina, K., Dunlea, E., Docherty, K., DeCarlo, P., Salcedo, D., Onasch, T., Jayne, J. T., Miyoshi, T., Shimono, A., Hatakeyama, S., Takegawa, N., Kondo, Y., Schneider, J., Drewnick, F., Borrmann, S., Weimer, S., Demerjian, K. L., Williams, P., Bower, K. N., Bahreini, R., Cottrell, L., Griffin, R., Rautiainen, J., Sun, J., Zhang, Y., and Worsnop, D. R.: Ubiquity and dominance of oxygenated species in organic aerosols in anthropogenically-influenced Northern Hemisphere midlatitudes, Geophysical Research Letters, 34, 2007.

Zhao, R., Mungall, E. L., Lee, A. K., Aljawhary, D., and Abbatt, J. P.: Aqueous-phase photooxidation of levoglucosan–a mechanistic study using Aerosol Time of Flight Chemical Ionization Mass Spectrometry (Aerosol-ToF-CIMS), Atmospheric Chemistry and Physics Discussions, 14, 8819-8850, 2014.

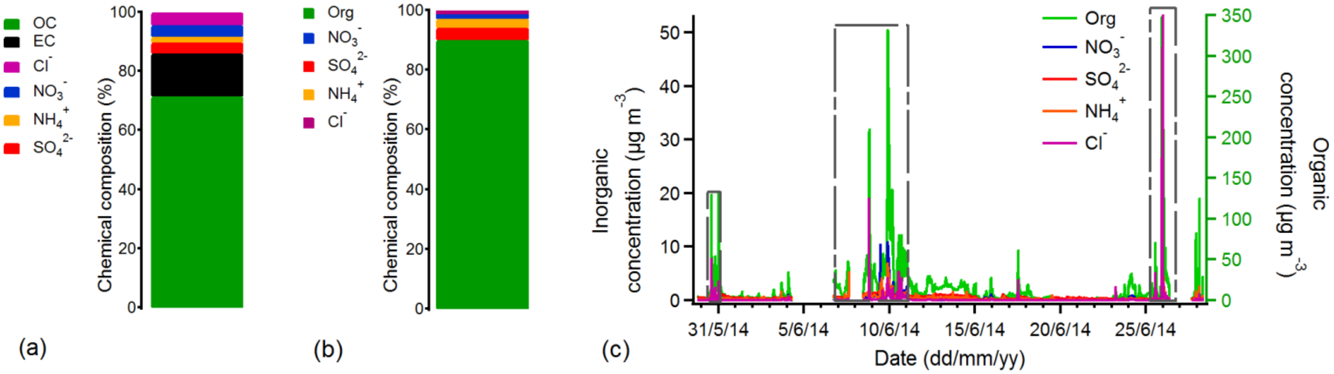

Figure 1: Contributions of (a) OC, EC and inorganics collected on filters and the contribution of (b) AMS ~~organic~~ OA and inorganics in non-refractory submicron aerosol ~~fraction~~, as well as (c) their time series. Close BB periods are marked in the AMS time series with grey dashed boxes. The distant BB periods cover all days of the measurement other than days included in close BB periods. Gaps in the AMS time series indicate gaps in the sampling.

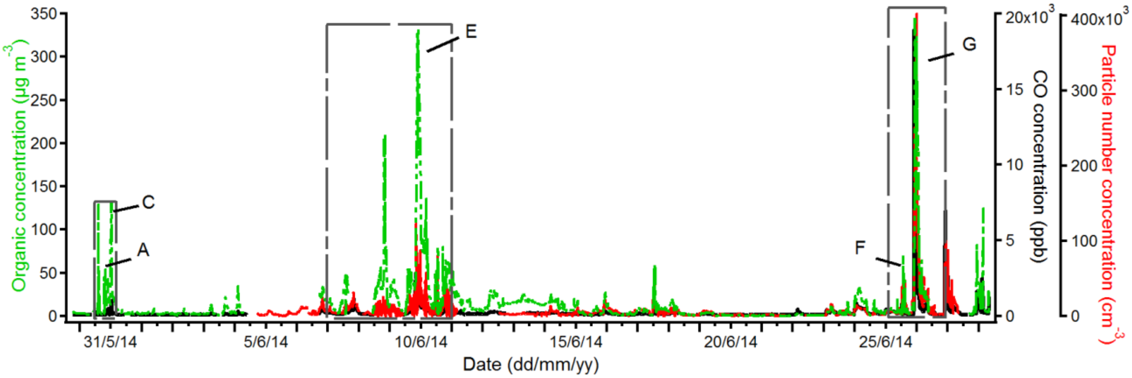

Figure 2: Time series for AMS ~~organics~~OA, CO and particle number concentration during the SAFIRED campaign. Close BB periods are marked with grey dashed boxes and selected BB events (A, C, E, F and G) are labelled. The distant BB periods cover all days of the measurement other than days included in close BB periods. Gaps in the time series indicate gaps in the sampling (no data for the instrument).

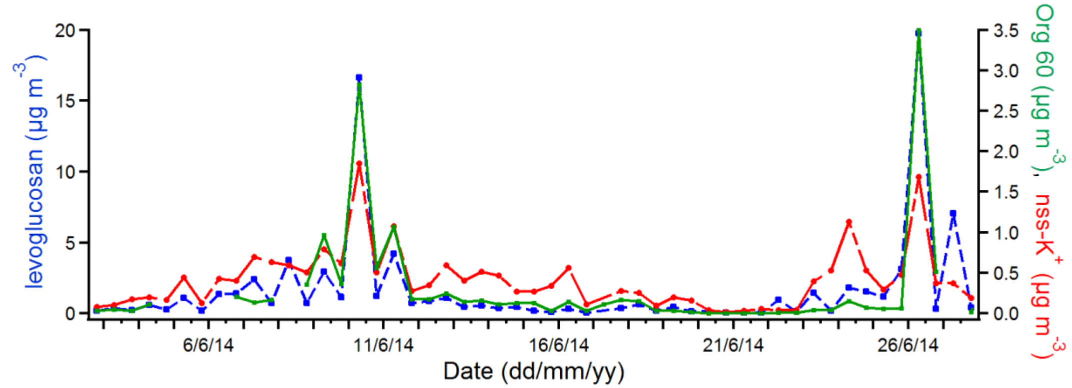

Figure 3: Time series of BB tracers: levoglucosan, soluble non-sea salt potassium (nss-K$^+$) (both 12h resolution) and AMS Org 60 (averaged to BAM 12h).

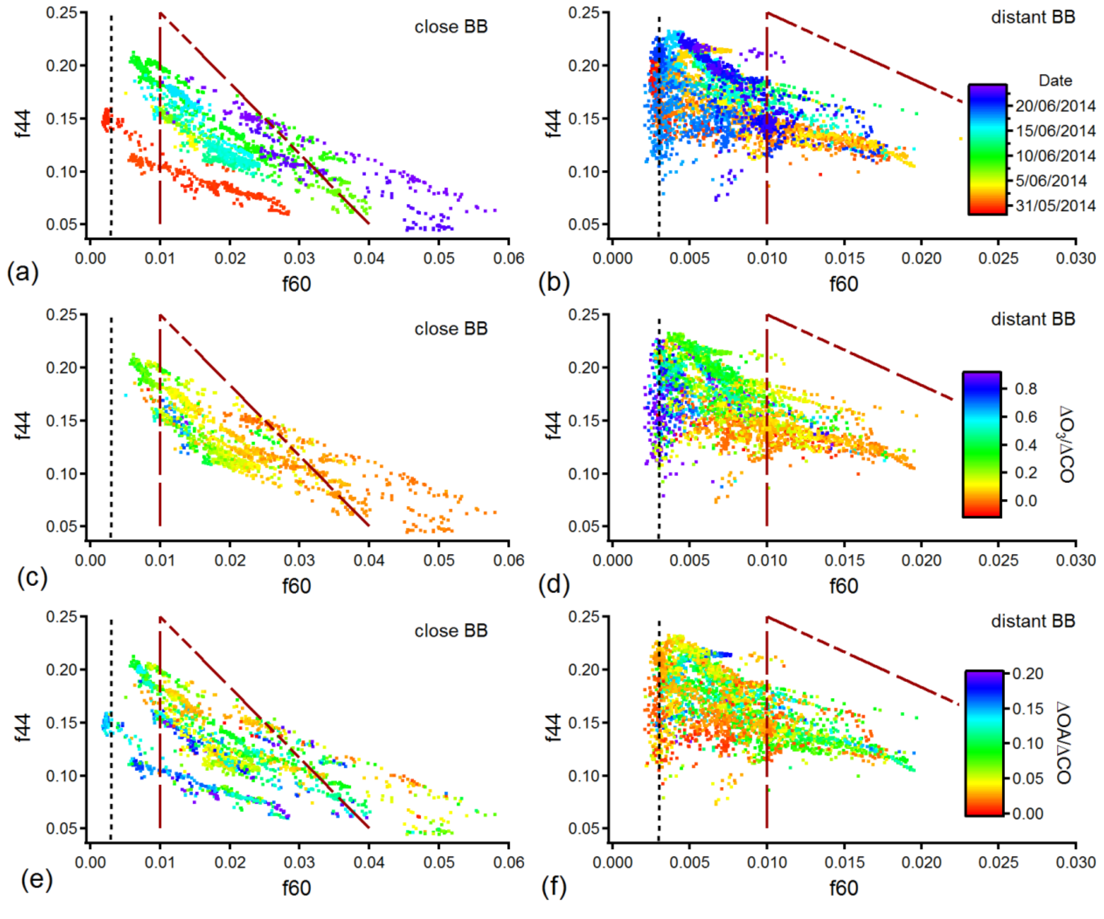

Figure 4: f44 vs. f60 coloured by date for (a) close and (b) distant BB periods, by ΔO$_3$/ΔCO ratio for (c) close and (d) distant BB periods, and by ΔOA/ΔCO ratio for (e) close and (f) distant BB periods (vertical dashed black lines refer to the f60 background level of 0.003). Red dashed lines refer to the ambient BBOA-related data space introduced by (Cubison et al., 2011). Note: ozone data from the 29th of May until the 1st of June were not available.

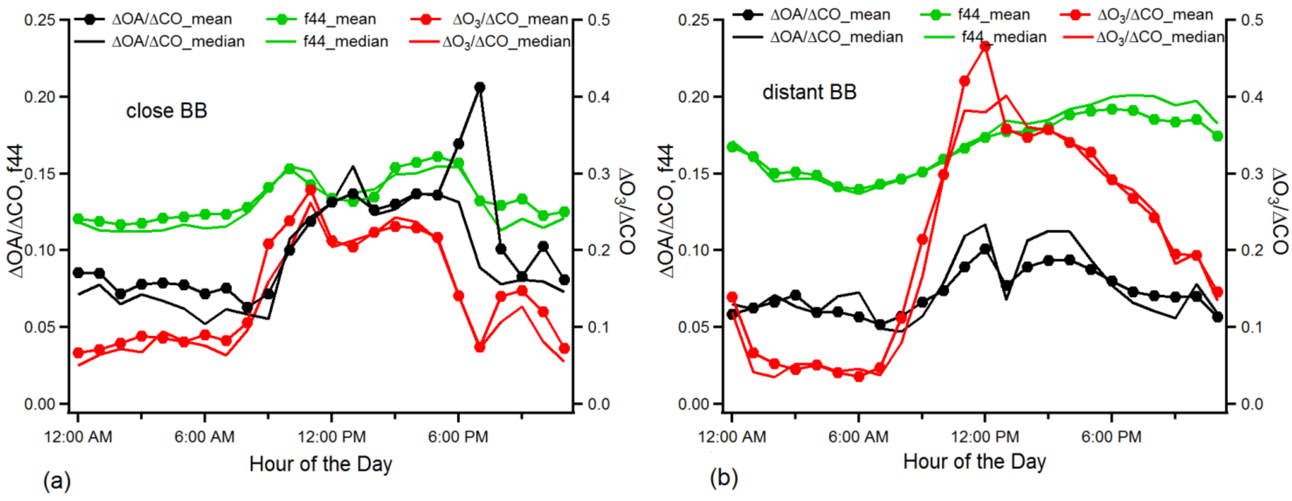

~~Figure 5: Diurnal trend of f44 (mean and median), $\Delta O_3/\Delta CO$ ratio (mean and median) and $\Delta OA/\Delta CO$ ratio (mean, median)for close (a) and distant (b) BB periods.~~

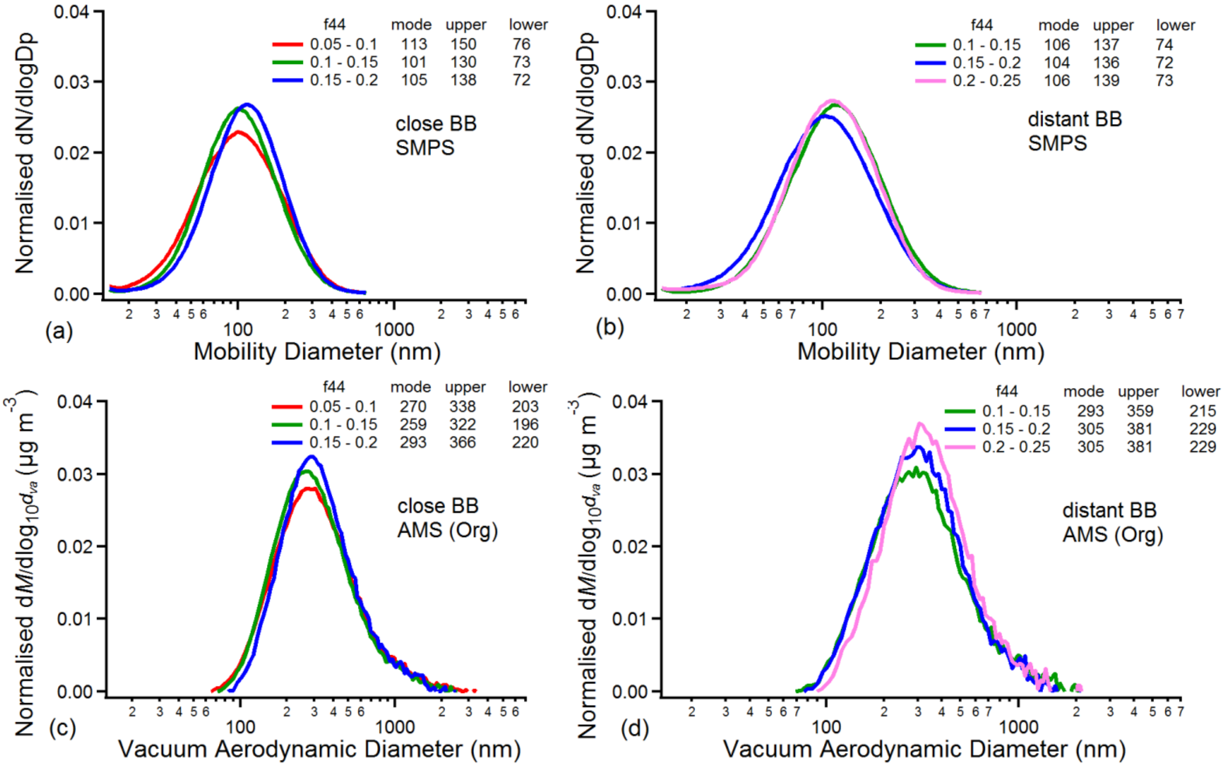

Figure ~~6~~5: SMPS size distributions (dN/dlogDp, normalised to total particle number concentration, versus mobility diameter) binned by the AMS f44 for close (a) and distant (b) BB periods and AMS size distributions ($dM/d\log_{10}d_{va}$, normalised to total ~~organic~~ OA concentration, versus vacuum aerodynamic diameter) binned by the AMS f44 for close (c) and distant (d) BB periods.

Table 1: Selected BB event values for f44, f60, ~~organic~~ OA concentration, CO, MCE, mode diameter and $\Delta O_3/\Delta CO$ ratios, along with measurement start and end time. ND refers to no data.

	Date (start/end)	f44±SD (range)	mean f60±SD (range)	mean Org±SD* (range)	mean CO±SD* (range)	MCE	$\Delta O_3/\Delta CO$	Mode diameter (nm)
A	30/05/14 18:34- 30/05/14 19:25	0.087±0.08 (0.079-0.105)	0.016±0.002 (0.010-0.018)	22.6±12.5 (4.6-45.2)	185.9±95.5 (90.2-370.1)	0.97± 0.06	ND	ND
C	30/05/14 23:41- 31/05/14/ 00:59	0.066±0.005 (0.060-0.079)	0.027±0.002 (0.021-0.028)	75.5±40.0 (13.7-131.2)	627.1±345.4 (185.8-1181.6)	0.98± 0.11	ND	ND
E	09/06/14 19:45- 10/06/14 00:32	0.078±0.013 (0.062-0.093)	0.032±0.002 (0.030-0.035)	175.9±105.0 (87.3-331.8)	1558.5±965.5 (671.6-3382.5)	0.91± 0.05	0.024	146
F	25/06/14 12:28- 25/06/14 16:59	0.134±0.031 (0.073-0.178)	0.009±0.002 (0.007-0.014)	13.2±14.5 (2.4-70.8)	479.0±348.8 (139.5-1642.7	0.93± 0.04	0.134	98
G	25/06/14 21:40- 26/06/14 03:59	0.062±0.017 (0.045-0.098)	0.046±0.004 (0.035-0.052)	144.6±104.7 (25.8-347.7)	2744.6±2299.8 (592.8-11275.7)	0.90± 0.06	0.011	88

*unit is µg m^{-3}

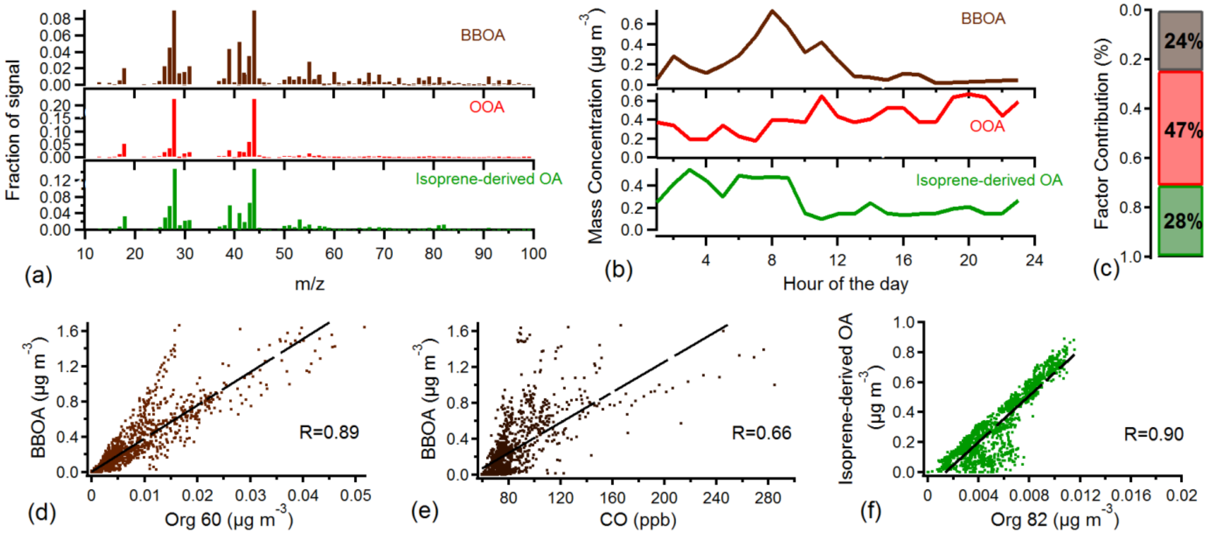

Figure ~~7~~6: (a) Mass spectra, (b) diurnal trends, (c) contribution and (d), (e), (f) correlations for the PMF 3-factor solution for background periods including BBOA, OOA and isoprene-derived OA factors.

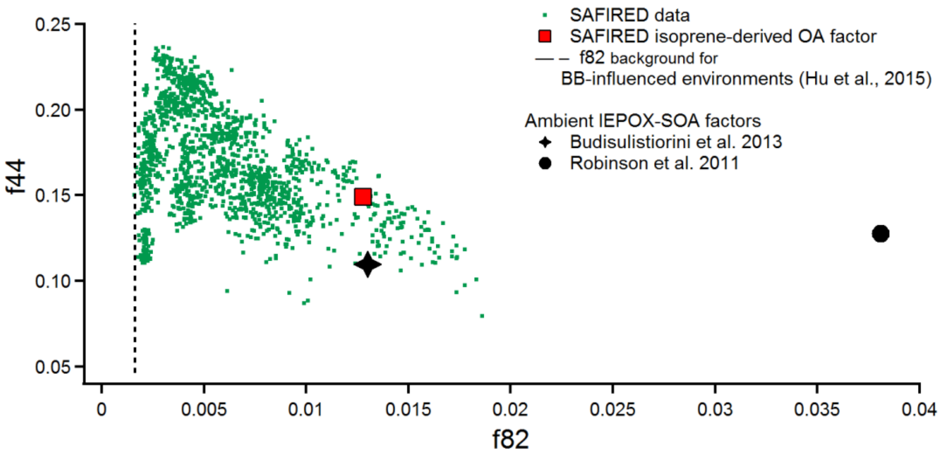

Figure ~~8~~7: f44 (CO_2^+) vs. f82 ($C_5H_6O^+$) for the SAFIRED data; The isoprene-derived OA factor from SAFIRED and two other ambient campaigns (Budisulistiorini et al., 2013;Robinson et al., 2011) are marked. Vertical black dashed line indicates proposed background f82 value in environments strongly influenced by BB (Hu et al., 2015).

S1 Data analysis

High organic aerosol (OA) loadings during heavy biomass burning (BB) episodes interfered with sulfate detection by the AMS in unit mass resolution (UMR), resulting in negative sulfate readings and scattered data points (Fig. S1a). Adjustments in Squirrel to the fragmentation table addressed the negative data points (Fig. S1b), however significant data dispersion still remained. High resolution (HR) fitting using PIKA improved correlation among different sulfate fragments (Fig. S1c).

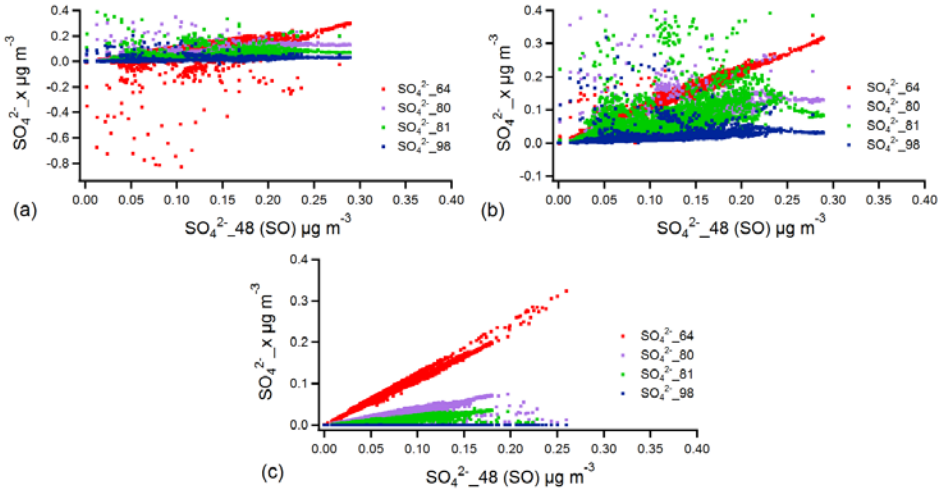

Figure S1: Sulfate fragments plots (a) before and (b) after Squirrel fragmentation table adjustments, and (c) after HR fitting in PIKA; SO_4^{2-}_x indicates sulfate fragments at m/z 64, 80, 81 and 96 plotted against the sulfate fragment at m/z 48.

PM1 soluble ions measured by ion suppressed chromatography and OM (converted from OC that was determined by the Thermal-Optical Carbon Analyser) were compared to the corresponding AMS UMR and HR data. A considerable improvement was observed in the HR analysis results for sulfate (Fig. S2b), with R changing from 0.4 to 0.8. HR fitting did not result in significant change for the other inorganic species or organics. However, improvement in the sulfate signals was significant and HR peak fitting data were used in further analysis.

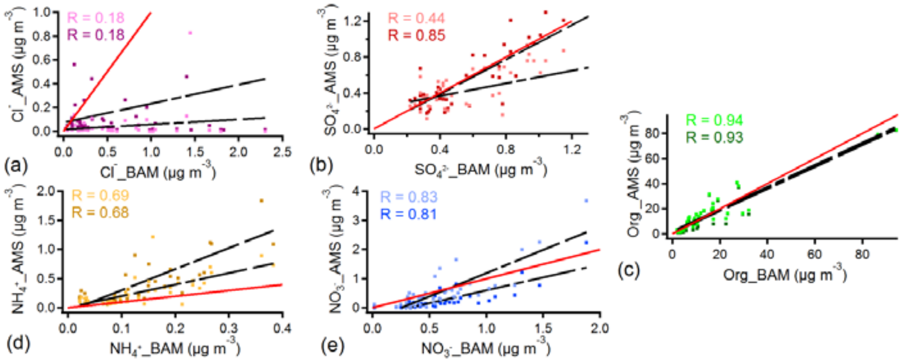

Figure S2: Correlation between BAM PM1 soluble ions and corresponding AMS species including (a) chloride, (b) sulfate, (c) ~~organics~~OA, (d) ammonia and (e) nitrate; The lighter points and first number present correlation of BAM data with UMR AMS data, while the darker points and the second number illustrates the correlation for BAM and HR AMS data. Red line represents 1:1 line (absolute concentration between AMS and BAM). BAM organic mass (OM) was converted from OC mass using the conversion coefficient of 1.4. R refers to Pearson correlation coefficient. The AMS data were averaged to BAM 12h data.

Table S1: Correlation values between inorganic species and ~~organics~~ OA during the campaign, and close and distant periods separately. Inorganic species measured during the whole period (X), close BB periods (X(c)) and distant BB periods (X(d)) were compared to ~~organics~~ OA measured during the same time period (Org, Org(c), Org(d)).

	Cl^-	Cl^- (c)	Cl^- (d)	NH_4^+	NH_4^+ (c)	NH_4^+ (d)	NO_3^-	NO_3^- (c)	NO_3^- (d)	SO_4^{2-}	SO_4^{2-} (c)	SO_4^{2-} (d)
Org	0.65			0.92			0.75			0.55		
Org(c)		0.67			0.92			0.72			0.49	
Org(d)			0.47			0.73			0.77			0.48

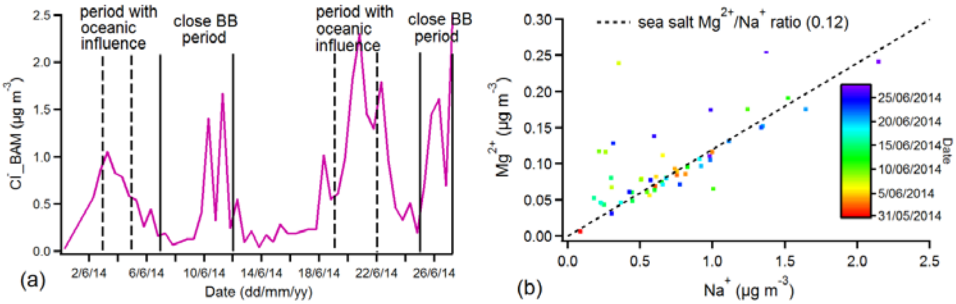

Figure S3: (a) Time series of chlorides collected on the filters (BAM). Dashed lines are defining the periods with oceanic influence, while solid lines illustrate close BB periods. (b) The filter (BAM) data for magnesium (Mg^{2+}) and sodium (Na^+). Black line illustrates Mg^{2+}/Na^+ ratio for the sea salt (0.12).

S2 Biomass burning aerosols and aging

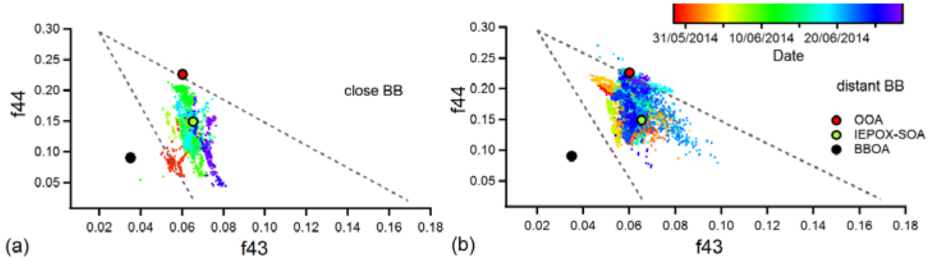

Figure S4: f44 vs. f43 coloured by date for (a) close and (b) distant BB periods. PMF-resolved factors are also indicated. The dashed lines represent boundaries for typical ambient aerosol as presented in Ng et al. (2010).

S2.1 Secondary organic aerosol (SOA) formation

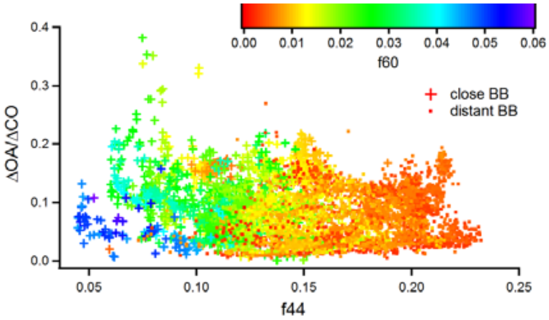

Figure S5: Change in ΔOA/ΔCO ratio with aging (represented by f44 values) for close (crosses) and distant (dots) fires coloured by f60.

S2.2 Biomass burning events

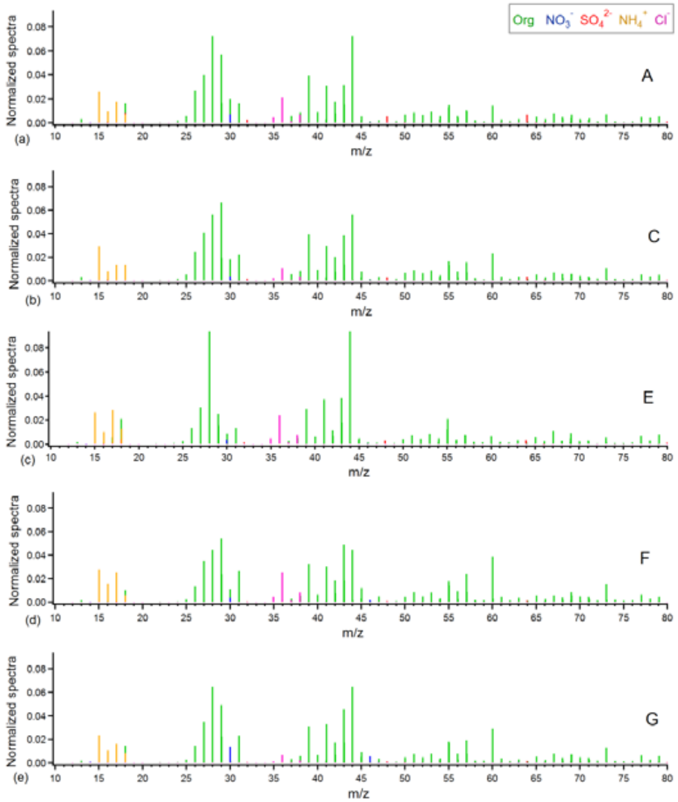

Figure S6: Normalised mass spectra (sum=1) for selected BB events (A (30/05/14, 18:34-19:25), C (30/05/14, 23:41-31/05/14 00:59), E (09/06/14, 19:45-10/06/14 00:32), F (25/06/14, 12:28-16:59) and G (25/06/14, 21:40-26/06/14 03:59) are shown respectively.

Sentinel hotspots and backtrajectories

On 30th of May at around 2pm three hot spots (two having confidence level of approximately 50% and one of 70%) were detected within 2km on the NE from the ATARS (Fig. S7a - Fig.S7d). These hot spots likely illustrated two fire events. On the same day and time, 11km on the SE from the sampling site, cluster of events was observed, including 4 hot spots with the confidence level between 94% and 100% and one of 78% confidence level. As all of them were spotted at the same time and within 1km distance, it is most likely that the one big fire has occurred. No other close events were observed over this time

Formatted: Heading 3

period. Cluster of hot spots was detected on the SE approximately 50km from the ATARS and big clusters at 100km and 150km, as well as on the SE. Moreover, 200km on E along the backtrajectories cluster of hot spots was observed.

On 25th of June three hotspot clusters were observed close to ATARS (2km on E, 5km on NE and 10km on SE) (Fig. S7e-Fig. S7h). The cluster of hot spots observed 10 km from the sampling site had one of the highest hot spot's power (energy released by the fire) observed close to the ATARS (within 20 km) during the campaign (120 MW/km^2). Besides the close fires two big clusters around 60 km and 120 km on the SE from ATARS were detected on the same day.

On the 9th of June cluster of hot spots (all with the confidence level higher than 70%) was detected 5 km from ATARS. Number of distant hot spots was detected between 100 km and 200 km, on the SE from the ATARS.

Formatted: Superscript

Backtrajectories for all BB Events are given at Fig. S7.

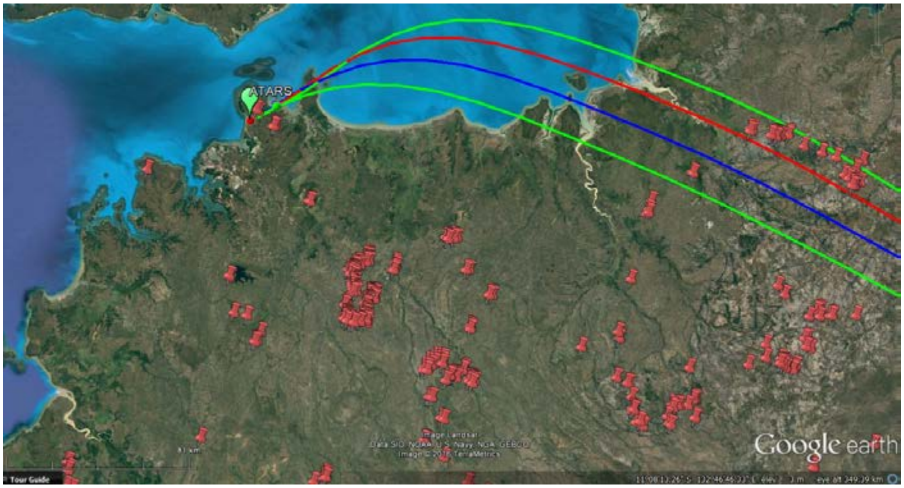

(a)


ATARS

(b)

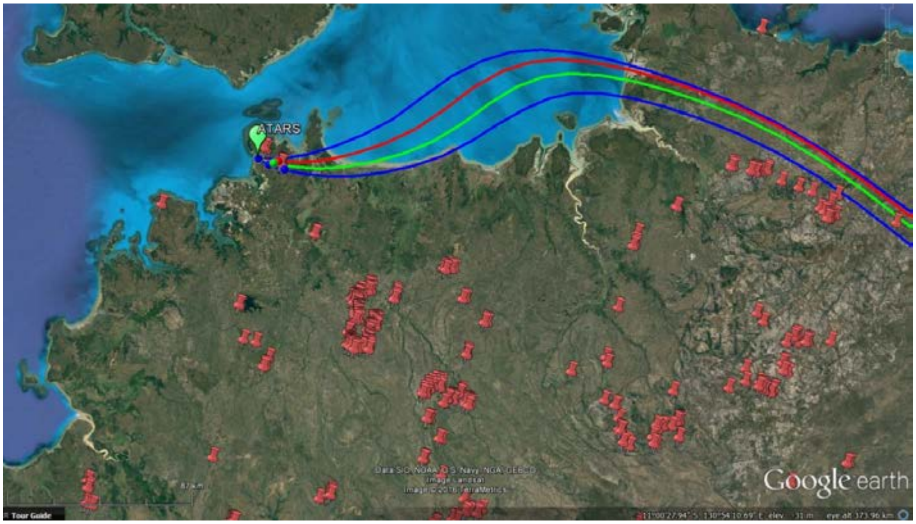
ATARS
Data SIO, NOAA, U.S. Navy, NGA, GEBCO
Image Landsat
Image © 2016 TerraMetrics
Google earth
Tour Guide
11°00'27.94" S 130°54'10.69" E elev 31 m eye alt 373.96 km

(c)

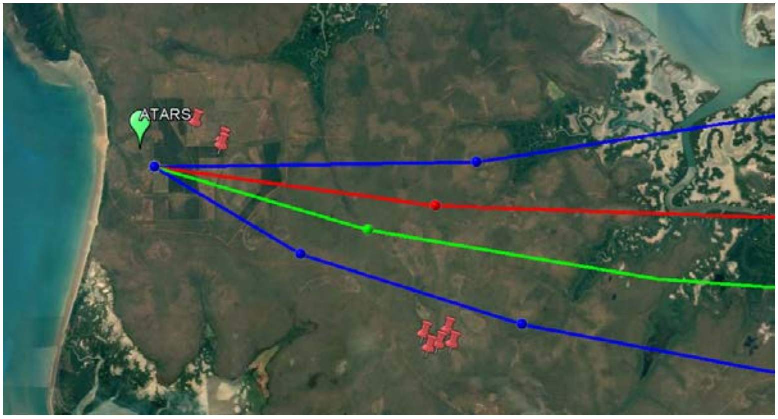
ATARS

(d)

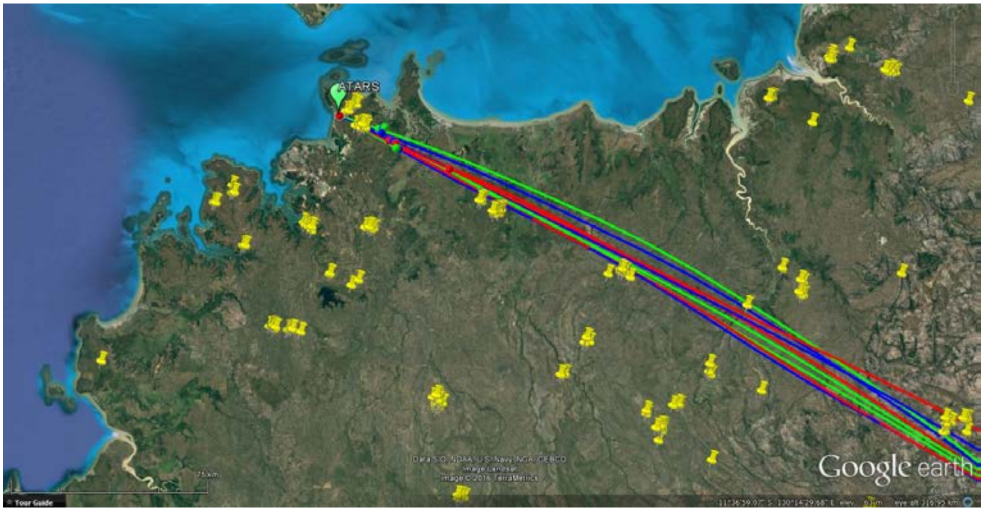
ATARS
Data S.I.O., NOAA, U.S. Navy, NGA, GEBCO
Image Landsat
Image © 2016 TerraMetrics
Google earth
75 km
Tour Guide

(e)

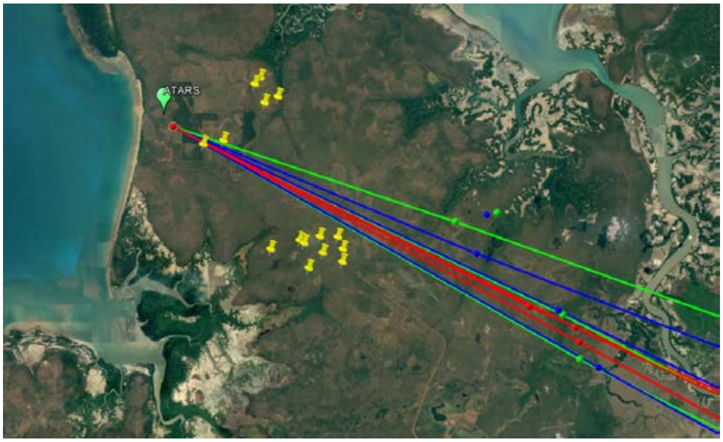
ATARS

(f)

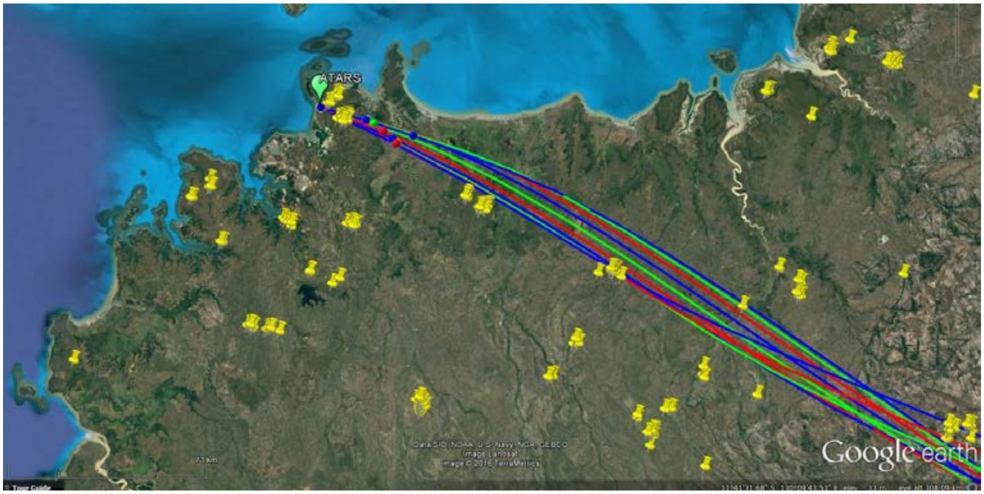
ATARS
Data SIO, NOAA, U.S. Navy, NGA, GEBCO
Image Landsat
Image © 2016 TerraMetrics
Google earth

(g)

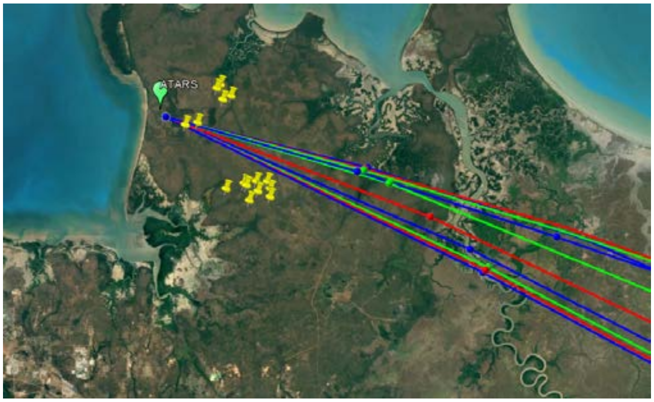
ATARS

(h)

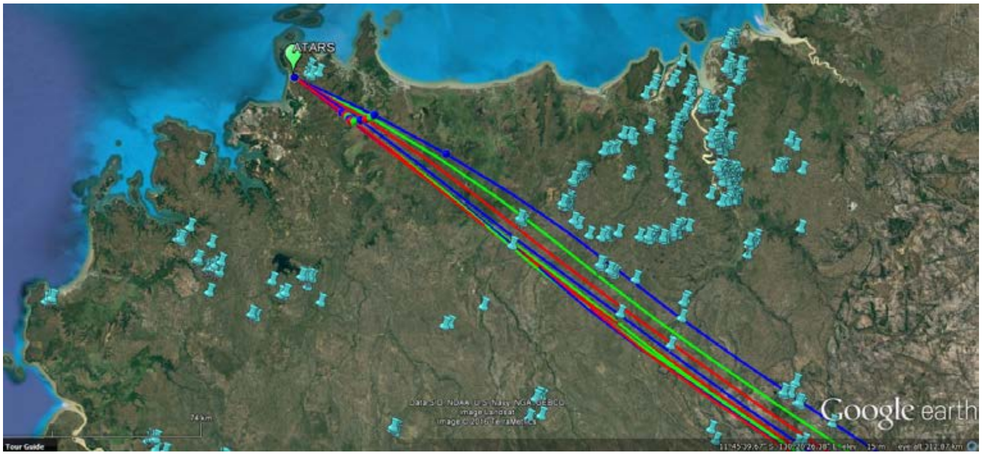
ATARS
Data SIO, NOAA, U.S. Navy, NGA, GEBCO
Image Landsat
Image © 2016 TerraMetrics
Google earth
74 km
Tour Guide
eye alt 212.07 km

(i)

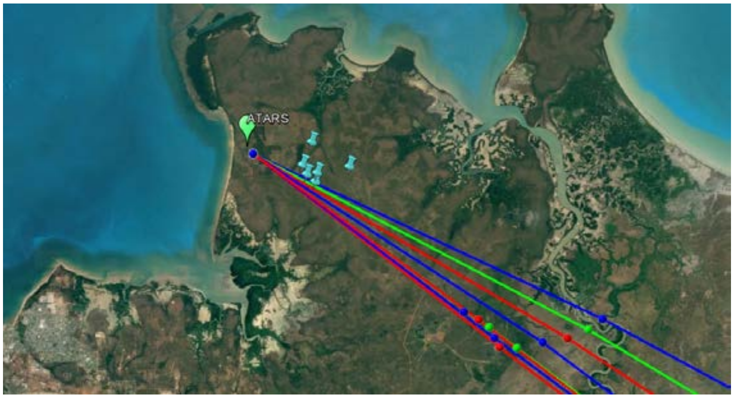

(j)

Figure S 7: Backtrajectories for ~~event~~ Event A, with close hot spots (a) and close and distant hot spots (b), for ~~event~~ Event C, with close hot spots (c) and close and distant hot spots (d), for ~~event~~ Event F, with close hot spots (e) and close and distant hot spots (f), for ~~event~~ Event G, with close hot spots (g) and close and distant hot spots (h) and for ~~event~~ Event E, with close hot spots (i) and close and distant hot spots (j). The backtrajectories were computed using the HYSPLIT (Hybrid Single-Particle Lagrangian Integrated Trajectory) model. All backtrajectories were run for 24h back in time. Different colours illustrate different starting time. (Google Earth V 7.1.2.2041; December 5, 2016; Northern Territory, Australia).

Formatted: Font color: Black

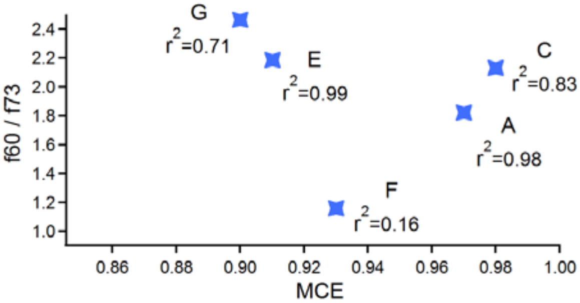

Figure S 8: f60/f73 ratio vs. modified combustion efficiency (MCE) for different events. Each point label indicates name of event and correlation value between f60 and f73.

S3 PMF performed on the whole dataset

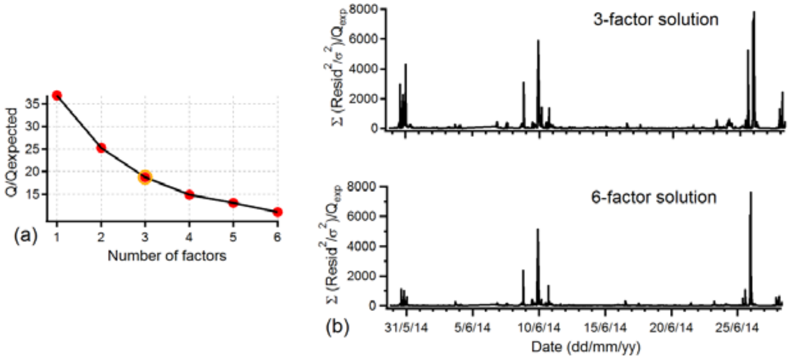

Figure S9: (a) Q/Qexpected (Q refers to the sum of squared scaled residuals over the whole dataset) vs. number of factors, illustrating high error and residual values. (b) Time series of Q/Q expected contribution for 3 and 6-factor solutions where it is clear that higher number of factors does not make the residual structure during BB events significantly lower.

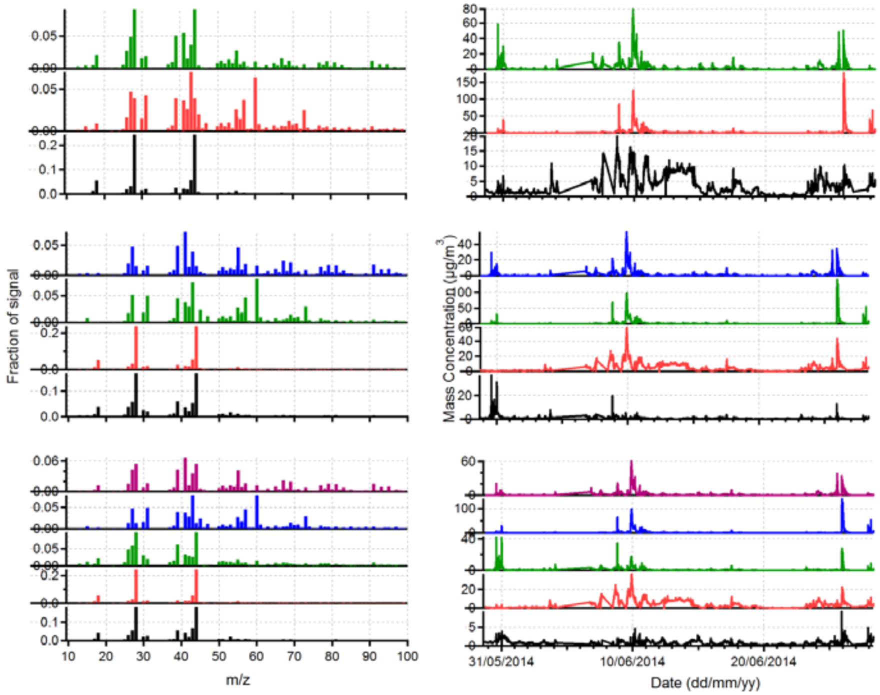

Figure S10: Factor profiles and time series for 3, 4 and 5-factor solutions showing BBOA factor splitting, suggesting that plumes are apportioned to different PMF factors.

S4 PMF performed on the background dataset

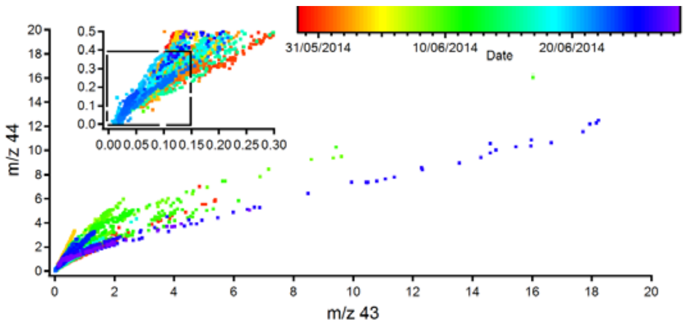

Figure S11: m/z 44 vs. m/z 43 coloured by date for the whole dataset and for background periods (inset). Black dashed box in inset graph illustrates cut-offs of 0.15 for m/z 43 and 0.4 for m/z 44 chosen for background data.

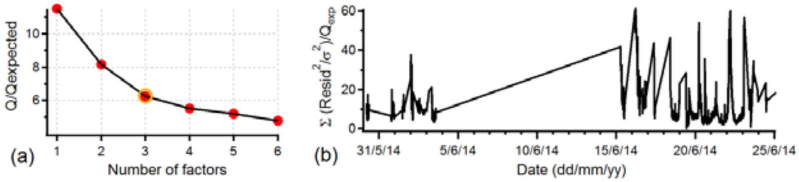

Figure S12: (a) Q/Qexpected vs. number of factors and (b) time series of Q/Q expected contribution for the 3-factor solution illustrating significantly smaller residuals in the case of the background dataset, compared to the whole dataset.

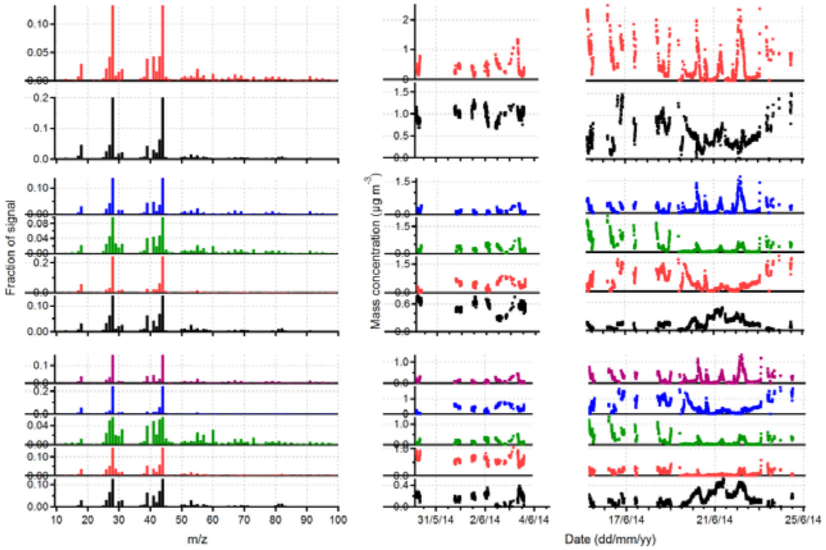

Figure S13: Factor profiles and time series for 2, 4 and 5-factor solutions for the background dataset.

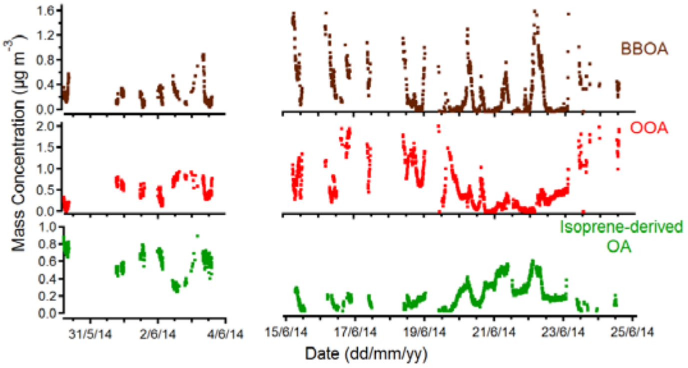

Figure S14: Time series for 3-factor solution for the background dataset.

S4.1 Isoprene-derived- organic aerosol

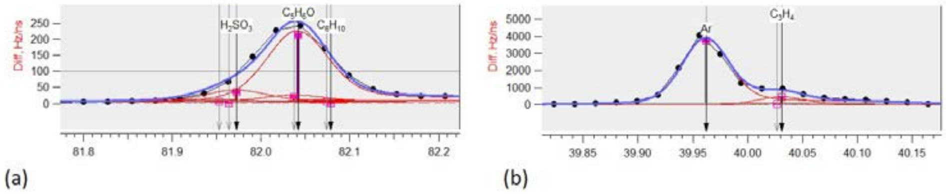

Figure S15: HR peak fitting at (a) m/z 82 showing the dominance of the $C_5H_6O^+$ fragment and (b) m/z 40 demonstrating good m/z calibration.

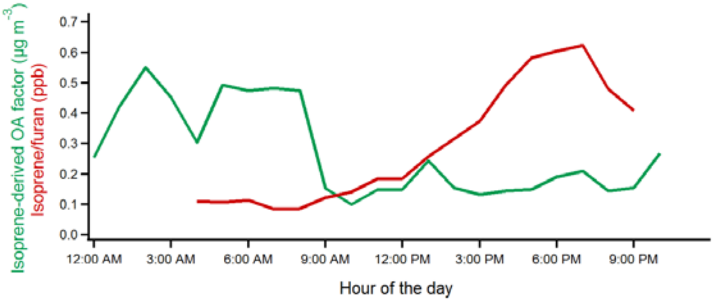

Figure S16: Diurnal trend of PMF IEPOX-SOA factor and isoprene/furan concentration measured by PTR-MS.

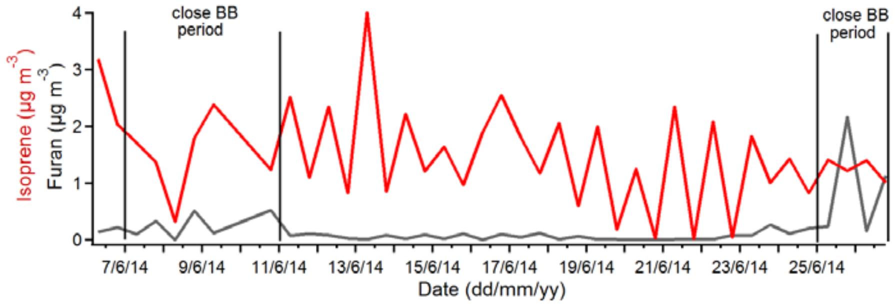

Figure S 17: Time series of isoprene and furan concentrations analysed by the gas chromatography-mass spectrometry. Black lines illustrate close BB periods.

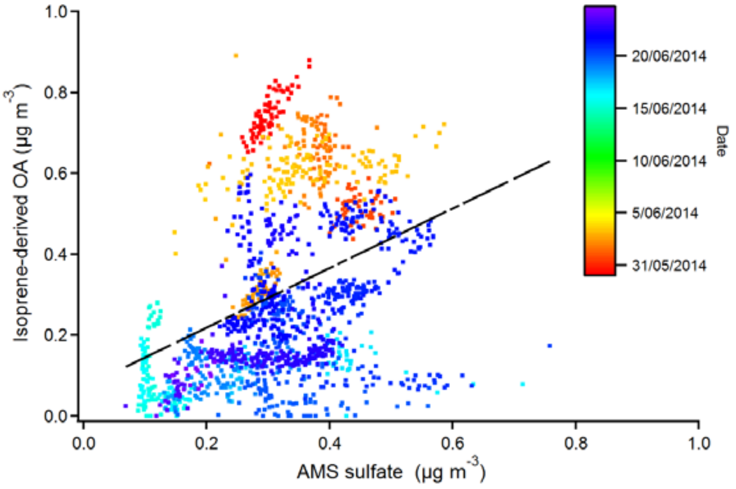

~~**Figure S 18: Correlation between of AMS sulfate with the isoprene-derived OA PMF factor.**~~